

الجمهورية الجزائرية الديمقراطية الشعبية
République Algérienne Démocratique et Populaire
وزارة التعليم العالي والبحث العلمي
Ministère de l'Enseignement Supérieur et de la Recherche Scientifique

جامعة غرداية

N° d'enregistrement

Université de Ghardaïa



كلية العلوم والتكنولوجيا

Faculté des Sciences et de la Technologie

قسم الآلية و الكهروميكانيك

Département d'automatique et d'électromécanique

Mémoire de fin d'étude, en vue de l'obtention du diplôme

Master

Domaine : sciences des matériaux

Filière : physique

Spécialité : physique des énergies et énergies renouvelables

Thème

Study and simulation of a tandem cell based on
hydrogenated amorphous silicon and its alloys

Présenté par :

GHOUL Fatma Zohra

Soutenue publiquement le..... /...../.....

Devant le jury composé de :

CHERIF Saleh	MCB	Univ. Ghardaïa	Président
MAIZ HADJ AMED Hamza	MAB	Univ. Ghardaïa	Encadrant
TAHTAH Reda	MAB	Univ. Ghardaïa	Encadrant
SEBA Hadj Yahia	MCB	Univ. Ghardaïa	Supervisor

Année universitaire/.....



Abstract

Abstract :

In this study, we simulate three amorphous silicon photovoltaic cells, the first is in hydrogenated amorphous silicon a-Si:H, the second is in hydrogenated amorphous silicon germanium a-SiGe:H and the third is a tandem cell in a-Si:H and a-SiGe: H. This simulation was carried out using the program AFORS-Het (Automated FOR Simulation of heterojunction). In this study, we focused on the effect of the thickness and doping concentration of each layer on the characteristics of photovoltaic cells (open circuit voltage, short circuit current, form factor and efficiency)

Keywords : Hydrogenated amorphous silicon ,Tandem cell, simulation ,AFORS -HET

Résumé :

Dans cette étude, nous simulons trois cellules photovoltaïques en silicium amorphe, la première est en silicium amorphe hydrogéné (a-Si:H), la seconde est en silicium germanium amorphe hydrogéné (a-SiGe:H) et la troisième est une cellule tandem en a-Si:H et a-SiGe:H. Cette simulation a été réalisée à l'aide du programme AFORS-Het (Automated FOR Simulation of heterojunction). Dans cette étude, nous nous sommes intéressés à l'étude de l'effet de l'épaisseur et de la concentration de dopage de chaque couche sur les caractéristiques des cellules photovoltaïques (tension de circuit ouvert, courant de court-circuit, facteur de forme

Les mots-clés : Silicium amorphe hydrogéné ,Cellule tandem ,simulation, AFORS-HET

ملخص

في هذه الدراسة، قمنا بمحاكاة ثلاث خلايا ضوئية من السيليكون غير المتبلور. الأولى في السيليكون غير المتبلور المهدرج a-Si:H، والثانية في السيليكون الجرمانيوم غير المتبلور المهدرج a-SiGe:H، والثالثة هي خلية ترادفية في a-Si:H و a-SiGe:H. تم تنفيذ هذه المحاكاة باستخدام برنامج (AFORS-Het المحاكاة الآلية للوصلات المتغيرة). في هذه الدراسة، ركزنا على تأثير سمك وتركيز تطعيم كل طبقة على خصائص الخلايا الضوئية (جهد الدائرة المفتوحة، تيار الدائرة القصيرة، عامل الشكل والكفاءة)

الكلمات المفتاحية: سيليكون غير متبلور مهدرج، خلية ترادفية، محاكاة، AFORS –HET



Dedication

And their final prayer is: "Praise be to Allah, the Lord of
all the worlds."

I dedicate this work to

To my mother and father, the apple of my eye, and my path to heaven. May Allah have mercy on
them as they raised me when I was young, and grant them abundant goodness and forgiveness.

O Generous, O Loving.

To those whom Allah Almighty mentioned, we will strengthen our bond with your brother.

To my sister and lifelong companion, Manal.

To my brothers, my support in this life, Yazid, Anouar, and Marouan Abdul Aziz.

To my grandfather, whose prayers brought me here.

And to all my family.

To the one who taught me the language of "Dhad" and the arithmetic, my dear teacher Fatima
Ousadiq.

To those I shared the sweetness of my academic journey and its hardships with, each of my
friends by name.

To Samer Redjeradj, my companion on the road and partner in beautiful and challenging moments
in university. The years of study were more beautiful with you.

To my dorm mates in A wing, who were like a family away from home.

To those who encouraged me in moments of weakness, who restored hope when it faded, I
dedicate this humble work.





Thanks and gratitude

I extend my sincere thanks and appreciation to my professor, [Seba hadj yahia], for his valuable guidance and continuous support. I also thank all the faculty members of [Mechanism and electromechanics] for the science and knowledge they provided.

I cannot fail to thank my colleagues and friends for their moral support.

I especially thank my dear family for their continued support.

May God reward everyone with the best reward.

[Ghoul Fatima Zahra]



List of figure, table and symbol

List of figure

Figure number	Content	Page number
Figure(1.1)	Types of solar radiation	6
Figure(1.2)	The visible part of the electromagnetic spectrum	7
Figure(1.3)	photoelectric cell	9
Figure(1.4)	p-type doping	10
Figure(1.5)	n-type doping	11
Figure(1.6)	p-n junction	11
Figure(1.7)	Photovoltaic effect in a silicon wafer	12
Figure(1.8)	Evolution of Solar Cell Efficiency Over the Years Taken from (NREL, 2024)	13
Figure(1.9)	Cell manufacturing stage: (1) Silicon ore – (2) refining (to increase purity) –(3) Molten silicon giving ingots (4) after solidification – (5) wafer obtained by sawing the ingot – (6) surface treatment by physicochemical processes and (7) finished cell with electrodes	13
Figure(1.10)	mono crystalline and poly crystalline cell	14
Figure(1.11)	Thin-layer solar cell	14
Figure(1.12)	(a) Crystal structure of silicon; (b) amorphous structure of silicon	18
Figure(1.13)	cell solar of pin photodiode	21
Figure(2.1)	equivalent diagram of the ideal solar cell	26
Figure(2.2)	Equivalent diagram of the solar cell	27
Figure(2.3)	represents the characteristic Current-Voltage (IV) curves for a solar cell in both under darkness and light exposure	28
Figure(2.4)	AFORS-HET program icon	31
Figure(2.5)	Graphical interface of the 1D simulation software AFORS-HET	32
Figure(2.6)	define structure of the solar cell	33
Figure(2.7)	Window of the structure of the solar cell	33
Figure(2.8)	introduction of the layer parameters	34
Figure(2.9)	Adding a layer	35

List of figure, table and symbol

Figure(2.10)	I-V characteristic and illumination	36
Figure(3.1)	Solar cell structure	39
Figure(3.2)	the evolution of the open circuit voltage V_{oc} (a), the short circuit current J_{sc} (b), the fill factor FF (c) and the efficiency η (d) as a function of the thickness of the absorber layer.	41
Figure(3.3)	Solar cell structure of a-SiGe:H	43
Figure(3.4)	the evolution of the open circuit voltage V_{oc} (a), the short circuit current J_{sc} (b), the fill factor FF (c) and the efficiency η (d) as a function of the thickness of the absorber layer	45
Figure(3.5)	Structure of tandem solar cells (a-Si:H,a-SiGe:H)	47
Figure(3.6)	the evolution of the open circuit voltage V_{oc} (a), the short circuit current J_{sc} (b), the fill factor FF (c) and the efficiency η (d) as a function of the thickness of the absorber layer	49
Figure(3.7)	the evolution of the open circuit voltage V_{oc} (a), the short circuit current J_{sc} (b), the fill factor FF (c) and the efficiency η (d) as a function of of doping the a-Si:H(n) layer N_D in a tandem solar cell	52
Figure(3.8)	the evolution of the open circuit voltage V_{oc} (a), the short circuit current J_{sc} (b), the fill factor FF (c) and the efficiency η (d) as a function of of doping the a-Si:H(p) layer N_a in a tandem solar cell	53

List of table

Table number	Content	Page number
Table(1.1)	wavelengths and frequencies of the solar spectrum	7
Table (3.1)	Cell-simulating physical constants	40
Table (3.2)	Cell-simulating physical constants	43
Table (3.3)	Cell-simulating physical constants	47

List of figure, table and symbol

List of symbol:

Symbol	Meaning	Unit
a-Si:H	Hydrogenated Amorphous Silicon	/
a-SiGe: H	Hydrogenated Amorphous Silicon-Germanium	/
a-SiC:H	Hydrogenated Amorphous Silicon-Carbide	/
NREL	National Renewable Energy Laboratory	/
PE-CVD	Plasma Enhanced Chemical Vapor Deposition	/
CdTe	Cadmium Telluride	/
CIS / CIGS	Copper Indium Gallium Selenide	/
TCO	Transparent Conductive Oxide	/
ITO	Indium Tin Oxide	/
CIGS	Copper indium gallium selenide	/
CVD	Chemical Vapor Deposition	/
S	Direct Radiation	/
D	Diffuse Radiation	/
G	Total Radiation	/
Voc	Open-Circuit Voltage	V
Isc	Short-Circuit Current	A
Pmax	Maximum Power Point	W
FF	Fill Factor	%
H	Solar Cell Efficiency	%
DC	Direct current	A
Dk	Dielectric constant	/
Chi	Electron Affinity	eV
Eg	Band Gap	eV
Eg opt	Optical Band Gap	eV
Nc	Effective Conduction Band Density	cm^{-3}

List of figure, table and symbol

Nv	Effective Valence Band Density	cm^{-3}
μ_n	Effective Electron Mobility	cm^2/V_s
μ_p	Effective Valence Band Density	cm^2/V_s
Na	Doping Concentration Acceptors	cm^{-3}
Nd	Doping Concentration Donors	cm^{-3}
Ve	Electron thermal velocity	Cm/s
Vh	Hole thermal velocity	Cm/s
Rho	Layer density	$g \times cm^{-3}$

Table of content

Table of Contents

Abstract	
Dedication	
Thanks and gratitude	
List of figure	
List of table	
List of symbols	
General introduction	1
Chapter one : generality about solar cell	4
1.1-Introduction:	5
1.2-The Sun:.....	5
1.3-Solar radiation :	5
1.3.1-Definition:.....	5
1.4-The solar radiation spectrum :	6
1.5-The definition of solar energy :	7
1.6-Material classification:	8
1.7-The doping :.....	8
1.8-The p-n junction:	9
1.9-Solar cells :	10
1.9.1-Definition :.....	10
1.9.2-The photovoltaic effect:	11
1.9.3-The different generations of photovoltaic cells:	12
1.9.3.1-First generation: silicon crystalline (mono and poly)	12
1.9.3.2-Second Generation solar cell (thin film):	14
1.9.3.3-Third generation solar cell:	16
1.9.4-Advantages and Disadvantages of Solar Cells:	16
1.9.4.1-Advantages of Solar Cells:.....	16

Table of content

1.9.4.1-Disadvantages of Solar Cells:	16
1.10-Amorphous Silicon and its Alloys :	17
1.10.1-Silicon and silicon alloys used in solar cells:	17
1.10.1.1-Structure et propriétés de silicium amorphe :	17
1.10.1.2-Doping of hydrogenated amorphous silicon :	19
1.10.1.3-Hydrogenated amorphous Silicon-Germanium alloy:	19
1.10.2-Single and multijunction solar cells based on amorphous silicon hydrogen:	20
1.10.2.1-Single junction solar cells:	20
1.10.2.2-Multijunction solar cells :	20
1.11-Conclusion:	21
Chapter tow: presentation of the simulation software	23
2.1-Introduction:	24
2.2-Simulation:	24
2.2.1-Definition:	24
2.2.2-Basic concepts in cell simulation:	24
2.2.2- Equivalent diagram of a solar cell:	25
2.2.3-Electrical Characteristics of the Solar Cell:[4]	28
2.2.4-The Current-Voltage (IV) characteristic curve :[1]	29
2.3-The electric model:[4]	29
2.4-Simulation software:	31
2.4.1-An overview of the AFORS-Het software:	31
2.4.2-Simulating the structure of a solar cell using the AFORS-Het software :	32
2.5- Conclusion:	37
Chapter Three: Results and discussion	39
3.1-Introduction:	40
3.2-Results and discussion:	40
3.2.1- The solar cell's particular structure of a-Si:H material:	40

Table of content

3.2.3- The effect of the thickness of the absorber layer on the cell properties:	42
3.2.4- The solar cell's particular structure of a-SiGe:H material:	43
3.2.5-Physical constants associated with each layer of the a-SiGe:H cell :	44
3.2.6-The effect of the thickness of the absorber layer on the cell properties:	45
3.2.7- The special structure of tandem solar cell (a-Si:H, a-SiGe:H):	47
3.2.8-Physical constants associated with each layer of the a-Si:H cell.....	48
3.2.9- The effect of the thickness of the absorber layer on the cell properties:	49
3.3 The effect of doping the a-Si:H(n) layer and a-Si:H(p) layer:.....	52
3.3.1-The effect of n-doping the a-Si:H(n) (the emitter) layer:	52
3.3.2-The effect of p-doping of the a-Si:H(p) (the base) layer:	53
3.4. Conclusion:	54
General conclusion	55
Sources and references.....	55



General introduction

fossil energies, such as oil, coal, and natural gas, are crucial energy sources heavily relied upon by the world. They are characterized by their ability to provide large quantities of energy efficiently, making them essential for industries, transportation, and electricity generation. However, their use poses environmental and economic challenges, such as environmental pollution and increased carbon dioxide emissions, alongside being finite resources that will deplete in the future. For these reasons, the world is shifting towards renewable energies like solar, wind, and hydropower to reduce dependence on non-renewable energies and ensure sustainable development while protecting the environment.

Solar energy is a renewable energy source that relies on sunlight. The sun is one of the richest sources of clean energy, contributing to reducing carbon emissions and environmental pollution. With technological advancements, solar panels and solar heating systems have become more efficient and effective. The efficiency of these systems depends on factors such as geographic location and climatic conditions. Investing in solar energy enhances energy security, creates job opportunities, and reduces reliance on fossil fuels.

Solar cells occupy a prominent position for offering clean and sustainable solutions. With continuous technological advancement, there is growing interest in developing solar cells with higher efficiency and lower cost. Among these developments are tandem solar cells that utilize various materials to improve energy conversion efficiency.

Amorphous silicon (a-Si:H) and its alloys represent a promising option for tandem solar cells. Amorphous silicon possesses unique properties that make it suitable for solar energy applications, such as low production costs and ease of manufacturing, in addition to the possibility of improving its efficiency through chemical composition modification with alloys like amorphous silicon carbide (a-SiC:H) and amorphous silicon germanium (a-SiGe:H).

This study aims to analyze and simulate the performance of tandem solar cells based on amorphous silicon and its alloys using the AFORS-HET program, which is specialized in modeling and analyzing solar cells and electronic devices with efficient energy applications. It is used to develop and improve solar cell designs by studying the factors affecting their performance, enabling researchers and engineers to develop more efficient techniques in the field of solar energy. By modeling these cells and studying the effects of various variables on their performance, the best configurations can be determined and tangible improvements i

efficiency can be achieved. This study will contribute to a deeper understanding of the physical and chemical properties of these materials and how to optimize their use in solar energy applications.

In our work, we will study the simulation of tandem solar cells made of amorphous hydrogenated silicon using the AFORS-HET program. We will address the following questions: What is the effect of variations in the absorber layer thickness and the concentration of dopants on the properties of the solar cell, represented by open-circuit voltage, short-circuit current, fill factor, and efficiency?

Chapter one provides an overview of solar cells, their different generations, and their key parameters. Additionally, it describes the characteristics of silicon-based amorphous solar cells.

Chapter two will delve into defining the physical constants associated with each layer for simulating a solar cell. Then, it will introduce the software ... and its usage method.

In chapter three, we present and discuss the main results found from the simulation. Finally, conclusions related to this study are drawn.



**Chapter one: generality about
solar cells**

Chapter one: generality about solar cells

1.1-Introduction

In this chapter, we will discuss the components and types of solar cells, the physical and chemical processes behind their work, how they are manufactured, and the latest trends and developments in this field, in addition to the challenges and opportunities facing this promising technology.

1.2-The Sun

It is one among the stars in the Milky Way galaxy, which has over 200 billion stars, and the center star of the solar system. At 1,392,684Km in diameter, the sun is roughly 109 times larger than the Earth. With a mass of 1030×2 kg, it is around 330,000 times heavier than the Earth. It is the main energy source that gives the planet heat and light. Like all stars, it is a giant sphere of heated gasses that, at its core, transforms hydrogen into helium to produce enormous quantities of energy.[1]

1.3-Solar radiation

1.3.1-Definition

It is the amount of solar radiation that reaches a specific area and is capable of generating electrical energy. Only a small fraction of solar radiation reaches the Earth, estimated to be about one part in a million of the total solar radiation, which is approximately 130 megawatts per square meter of the Sun's surface. This small quantity is responsible for all the thermal energy on the Earth's surface and in its atmosphere.[1]

This radiation penetrates the Earth's atmospheric envelope, and part of it reflects outside the atmosphere into space, while the rest scatters inside the envelope. The remaining part passes through the envelope, and thus solar radiation reaches the Earth's surface in three forms:

- a- Direct Radiation (S): This is the radiation that passes through the atmosphere without reflection or scattering, consisting of a direct beam of sunlight that arrives unchanged.
- b- Diffuse Radiation (D): This is the radiation that undergoes scattering by atmospheric components.
- c- Total Radiation (G): This is the radiation that reaches a point on the Earth's surface and consists of the sum of direct, diffuse, and reflected radiation, calculated as follows:

$$G=R+S+D$$

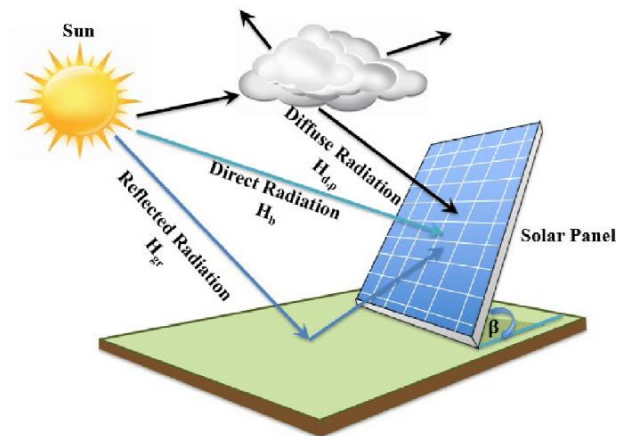


Figure (1-1): Types of solar radiation [2]

1.4-The solar radiation spectrum

The solar radiation spectrum encompasses a diverse range of electromagnetic wavelengths emitted by the sun. This spectrum comprises several key elements, including visible light, which is perceivable by the human eye; ultraviolet radiation, characterized by high energy and potential harm to human health; infrared radiation, felt by humans as heat without being visible; and radio waves, distinguished by much longer wavelengths than infrared radiation, which are neither visible nor perceptible by the human eye. Most of the solar radiation spectrum reaches the Earth's surface unchanged, although a portion is absorbed as it passes through the atmosphere. Additionally, the sun not only produces visible, infrared, and ultraviolet radiation from the solar spectrum colors but also emits high-energy gamma rays as a result of nuclear fusion processes occurring in its core.[1]

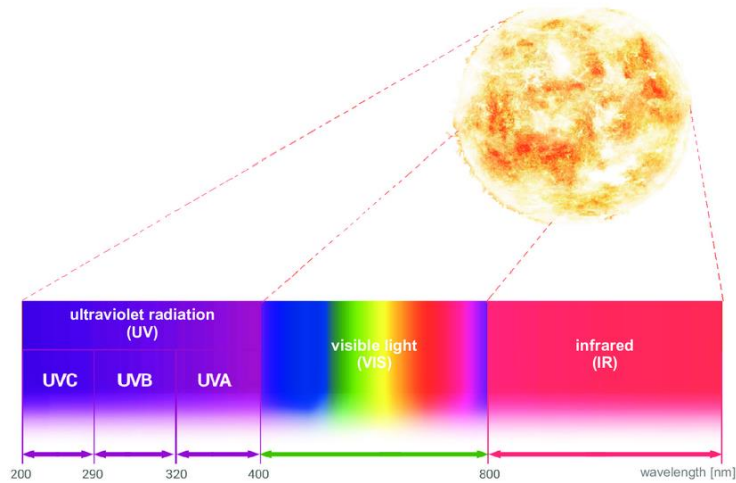


Figure (1-2) The visible part of the electromagnetic spectrum [3]

Table 1-1: wavelengths and frequencies of the solar spectrum [4]

Différents rayons	Longueurs d'onde	Fréquences
Ultraviolets	100-400 nm	3000-750 THz
Visibles	400-780 nm	750-385 THz
Infrarouges	780-10 ⁶ nm	385-0,3 Thz

1.5-The definition of solar energy

It is the energy that is derived from the sun, which consists of using the light and heat that is emitted from the sun to generate electricity, heat water, or for other purposes. Solar energy is a clean and renewable source of energy, which is generated using various solar technology such as solar cells and solar mirrors. Solar energy is considered one of the most important energy sources available in the world, and it depends on taking advantage of the sun's radiation that reaches the Earth's surface to generate energy.[1]

Solar energy can be converted into thermal energy and electrical energy:

Thermal energy: It is obtained by the heat conversion mechanism, which depends on Converting solar radiation into thermal energy through solar collectors. If a dark-colored,

Chapter one: generality about solar cells

isolated body is exposed to solar radiation, it absorbs the radiation and its temperature rises. It benefits from This heat is used in heating, cooling and water heating.

Electrical energy: We obtain this energy through the photoelectric conversion mechanism, which It means converting solar radiation directly into electrical energy using solar cells.

1.6-Material classification

Materials are divided according to their ability to conduct electrical current into three main types:

a-conductors: These are materials that allow electrical current to flow easily. It is characterized by the presence of free electrons roaming within the structure of matter, such as silver, copper, aluminium, gold, and iron.

b-Insulators: These are materials that do not allow electric current to flow. It is characterized by the absence or scarcity of free electrons within the structure of matter. Such as plastic, wood, glass and air.

c-Semiconductors: These are materials with moderate electrical conductivity, located between conductors and insulators. It is characterized by the presence of a limited number of free electrons. The conductivity of a semiconductor can be changed by adding impurities to it (doping). Examples of semiconductors are silicon, germanium, and gallium arsenide.[1]

1.7-The doping

Doping is the process of introducing impurities into a pure semiconductor material to alter its electrical conductivity. These impurities, known as dopants, are typically elements from groups III and V of the periodic table. [1]

There are two main types of dopants: N-type and P-type. N-type dopants, such as phosphorus, arsenic, and antimony, contain five valence electrons. When added to a pure semiconductor, they donate an extra electron, creating free electrons that contribute to conductivity. On the other hand, P-type dopants, such as boron, aluminum, and gallium, contain three valence electrons. When added to a semiconductor, they create holes in the electron structure, which act as charge carriers and contribute to conductivity.

Chapter one: generality about solar cells

Doping significantly enhances the electrical conductivity of semiconductors by providing additional charge carriers. N-type and P-type semiconductors have different electrical properties due to their distinct doping mechanisms.

Doped semiconductors form the foundation of modern electronic devices, including transistors, diodes, and integrated circuits. Controlled doping enables precise customization of semiconductor properties, allowing these devices to perform a wide range of functions.

The doping process involves adding a small amount of dopant material during the crystal growth of semiconductors. The dopant atoms are incorporated into the semiconductor's crystalline lattice, altering its electronic properties and conductivity its electronic properties and conductivity [1]

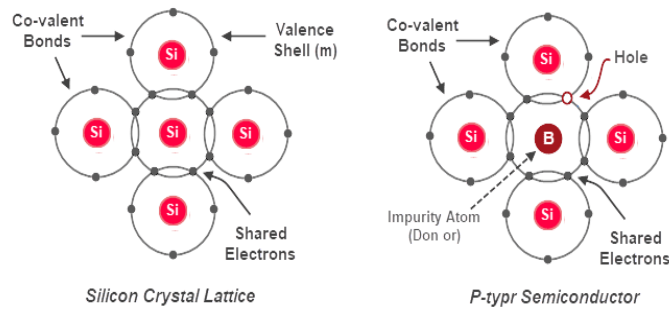


Figure (1.3):p-type doping[6]

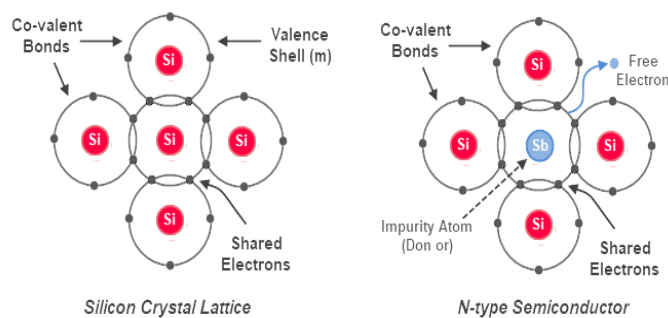


Figure (1.4): n-type doping [6]

1.8-The p-n junction

Chapter one: generality about solar cells

The p-n junction diode is formed by joining a pure semiconductor with one end doped with a pentavalent impurity (rich in free electrons), resulting in an N-type semiconductor, and the other end doped with a trivalent impurity (rich in free holes), resulting in a p-type semiconductor. When these two regions are connected at the junction area, negative charges from the N-type region migrate and combine with the holes in the P-type region, creating a depletion region. This forms a diode, symbolized as a symbol in electronic circuits, allowing current to flow in one direction while blocking it in the reverse direction.

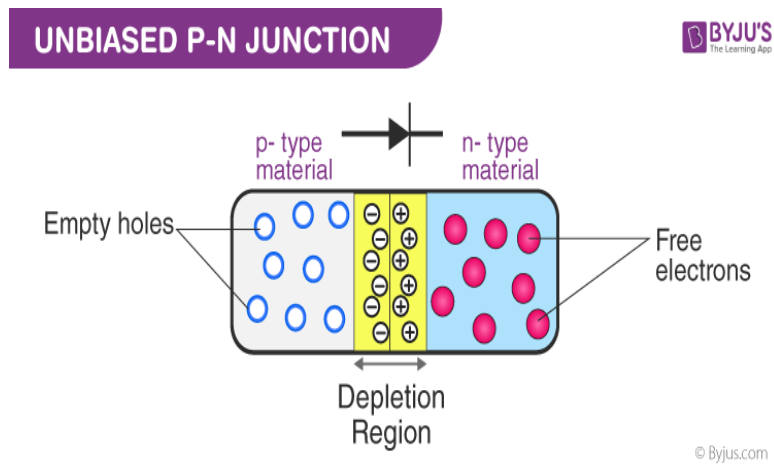


Figure (1-5) p-n junction [7]

1.9-Solar cells

1.9.1-Definition

A solar cell is an electronic device that converts direct sunlight into electrical energy using the phenomenon of internal photoexcitation. Solar cells typically consist of semiconductor materials such as silicon and comprise two opposing conductive layers with an applied electric field between them. When sunlight strikes these cells, electrons are released in the active conductive layer, resulting in the flow of electrical current. Solar cells can be used to generate electrical energy in a variety of applications, including solar power generation on surfaces, powering standalone electronic devices, and providing energy for electric vehicles.

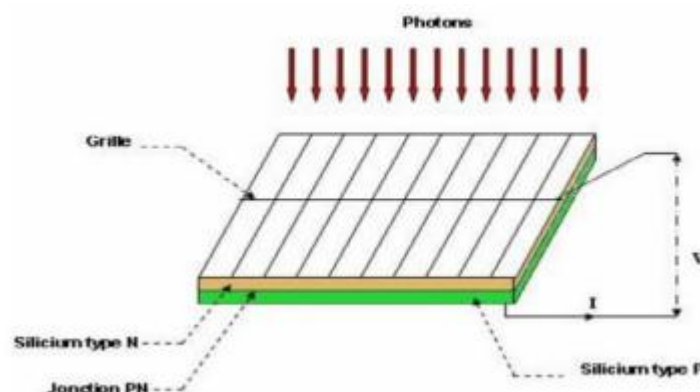


Figure (1.6): photoelectric cell [5]

1.9.2-The photovoltaic effect

The process by which light energy in a semiconductor is directly converted to electrical energy is known as the photovoltaic effect. A silicon wafer (semiconductor) that has been doped with phosphorus (N side) in the bottom section and boron (P side) in the top part is often used in solar cells.

An electric field keeps the electrical charges apart in the area around this P-N junction. An electron-hole pair is created when a photon strikes a cell and uses the photoelectric effect to break off electrons. The electron is gathered on the N side after having enough energy to pass the junction. A current of electricity is produced [4]



Figure(1.7): Photovoltaic effect in a silicon wafer [4]

1.9.3-The different generations of photovoltaic cells

The last several decades have seen the development of numerous innovative kinds of solar cells. Solar cells come in three generations. The many solar systems that have emerged from international research are shown in Figure 1.7, along with the top power conversion efficiencies from 1976 to 2024. A data table was created by the US Department of Energy's National Renewable Energy Laboratory (NREL). Over time, the power conversion efficiency of different kinds of solar cells has gone up. The type of material, the highest degree of performance that can be attained, and the cost of each kind decide which categories are used.[8]

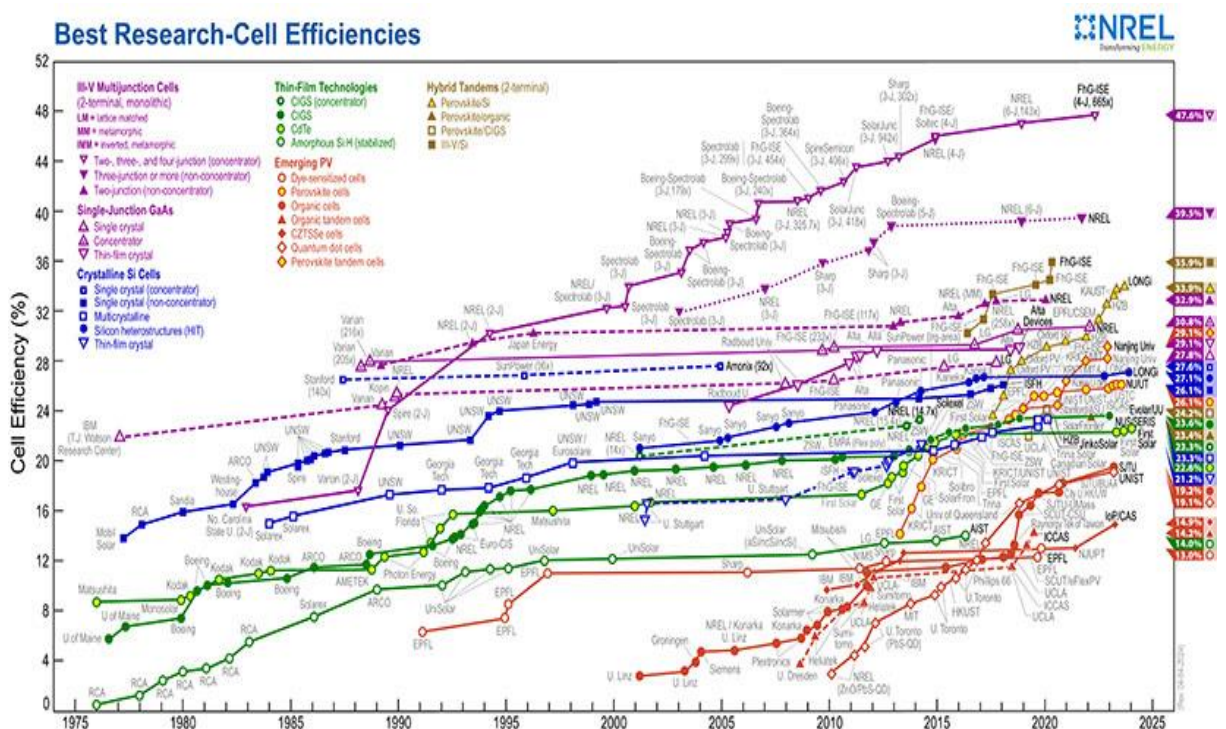


Figure (1-8): Evolution of Solar Cell Efficiency Over the Years Taken from (NREL, 2024) [9]

1.9.3.1-First generation: silicon crystalline (mono and poly)

This generation of cells is based on crystalline silicon wafers, which are thin slices that are sawed into silicon ingots. The purification process results in a material that has 99.99999% silicon.[10]

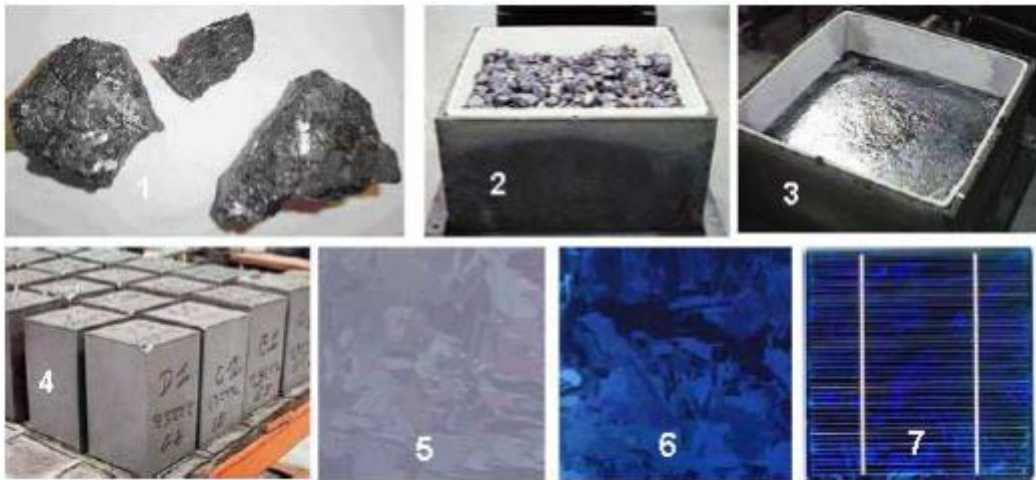
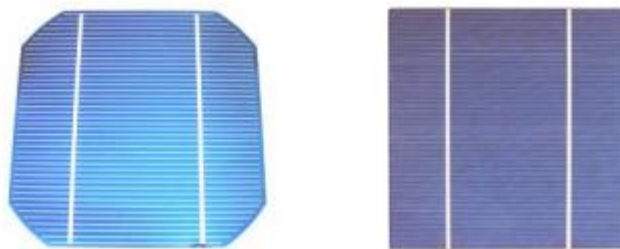


Figure (1.9): Cell manufacturing stage: (1) Silicon ore – (2) refining (to increase purity) –(3) Molten silicon giving ingots (4) after solidification – (5) wafer obtained by sawing the ingot – (6) surface treatment by physicochemical processes and (7) finished cell with electrodes [10]

Depending on the kind of structure, crystal cells are separated into two categories: mono- and polycrystalline. These two cell types—the Siemens process and the Czochralski (Cz) process—are the result of distinct solidification and purification procedures. The industries that typically carry out the purifying processes Cz and Siemens differ in their supply structures.



Figure(1.10): mono crystalline and poly crystalline cell[10]

Monocrystalline cells are distinguished by their broken corners and uniform appearance. THE poly-crystalline cells have a more iridescent appearance coming from the orientation of the different crystal lattices relative to the cutting plane.

1.9.3.2-Second Generation solar cell (thin film)

The basis for this generation of cells is the thin-film (or layer-thin) deposition of semiconductor materials. These substances are applied to a substrate using techniques like PE-CVD (Plasma Enhanced Chemical Vapor Deposition). The layer has a thickness that ranges from a few nanometers to tens of micrometers. Due to their lower weight per watt peak at launch, these once-expensive technologies were only used in concentrated and space applications. The cost of these technologies has decreased to the point where they are now competitive with first-generation crystalline technologies due to the increase in production volumes. Among the industrially utilized thin-film technologies (mass manufacturing), we separate:[10]

CdTe: Cadmium Telluride (cadmium teluride)

CIS / CIGS: Copper Indium Gallium Selenide

Thin film silicon: amorphous silicon α Si and microcrystalline

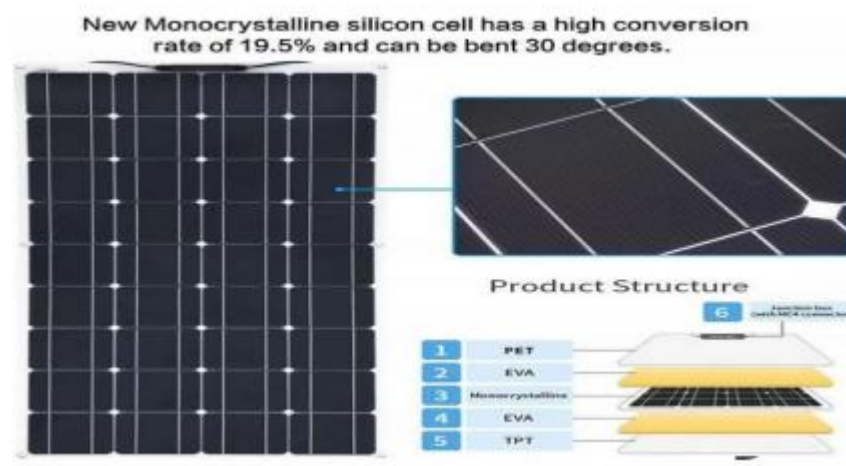


Figure (1.11): Thin-layer solar cell [1]

1.9.3.2.1-The basic elements of a thin film solar cell include

1-Substrate: This is the fundamental layer of the solar cell, serving as both a surface for the deposition of thin film layers and a mechanical support. Typical substrate materials include of plastic, metal, or glass.

Chapter one: generality about solar cells

2- Transparent conductive layer: In order to create a conductive path for current to flow in the solar cell and allow light to pass through to the active layers, this layer often consists of transparent conductive oxides like TCO and ITO

3-The active layer: This layer is composed of a semi-conducting material, like copper indium gallium selenide (CIGS), amorphous silicon, or cadmium telluride (CdTe), which absorbs photons from sunlight and produces an electrical charge. The active layer is typically only a few micrometers thick.

4- Back contact: This layer usually consists of a metal such as aluminum or silver, providing a secondary conductive path for current flow in the solar cell. It also reflects any unused light back through the active layer to increase the efficiency of the solar cell.

1.9.3.2.2- Advantages and disadvantages of thin film solar cells

a- Advantages:

- Mass production is simple and cost-effective, making them cheaper to manufacture than crystalline silicon solar cells.
- Their homogeneous appearance makes them more aesthetically pleasing.
- They offer flexibility, opening up possibilities for various new applications.
- They tolerate and produce energy in high-temperature environments, and shading has less impact on their performance.

b- Disadvantages:

- Generally, thin-film solar panels are not suitable for residential applications. While they are cost-effective, they also require a large area.
- Thin-film solar panels tend to degrade faster than monocrystalline and polycrystalline solar panels, which is why they usually come with shorter warranties compared to other types of solar panels.

1.9.3.3-Third generation solar cell

Mainly, due to the high costs of first generation solar cells and the toxicity and limited availability of materials for second generation solar cells, a new generation of solar cells has emerged. This is inherently different from the previous two generations because it does not depend on the p-n junction design of the others. The objective is of course to improve solar cells by making solar energy more efficient over a wider band of solar energy, cheaper and without any toxicity, in order to achieve these efficiencies, many concepts have been studied during the last years. This generation of solar cells includes organic thin film (polymer solar cells), dye-sensitized solar cells, perovskite solar cells and quantum dot solar cells

1.9.4-Advantages and Disadvantages of Solar Cells

1.9.4.1-Advantages of Solar Cells

- Renewable energy source.
- Reduces electricity consumption and lowers bills.
- Protects the environment from pollution.
- Provides long-term energy.
- Versatile applications.
- Low maintenance costs.
- Advances technology.

1.9.4.1-Disadvantages of Solar Cells

- Cannot fully meet internal needs (difficult to use solar cells in shaded areas).
- High initial cost.
- Seasonal energy production dependent on weather.
- Expensive energy storage.
- Requires a large amount of space.

1.10-Amorphous Silicon and its Alloys

1.10.1-Silicon and silicon alloys used in solar cells

1.10.1.1-Structure et propriétés de silicium amorphe

Amorphous silicon, a material with unique properties, has gained significant interest in the field of amorphous semiconductors due to its economic advantage and unique properties. Despite some disadvantages such as lack of reproducibility, low mobilities, and high defect densities, amorphous silicon can be a cost-effective replacement for crystalline silicon. Amorphous silicon does not have an organized structure, with small variations in length and angle of connection, resulting in conduction and valence band tails in the material's density. Defects in amorphous silicon are present in the form of silicon atoms with only three covalent bonds with neighbors, and the fourth unsatisfied link is called dangling links.

The concentration of dangling bonds in non-hydrogenated amorphous silicon is around 10^{19} to 10^{20} cm^{-3} , making it difficult for electronic applications. However, these dangling bonds can be easily passivated by a hydrogen atom, reducing the concentration of dangling bonds to approximately 10^{15} to 10^{16} cm^{-3} .

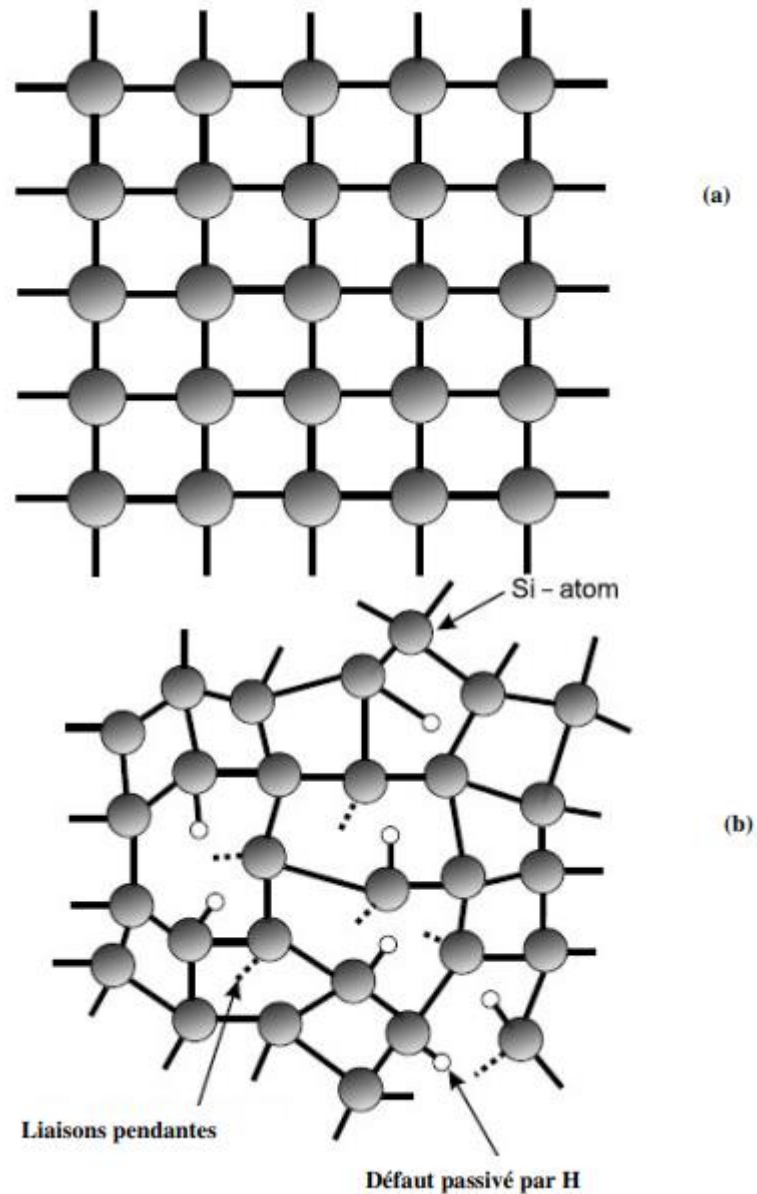


Figure 1.12:(a) Crystal structure of silicon; (b) amorphous structure of silicon.[11]

The electron's mobility gap, which signifies the energy difference between the valence band (E_v) and the conduction band (E_c) where electrons are immobile, typically ranges between 1.9 eV and 1.83 eV. This gap determines the minimum energy required for photons to be absorbed and contribute to photovoltaic conversion. In the case of a-Si:H, it behaves as a direct gap semiconductor, making it particularly efficient in absorbing visible light.

Moreover, a-Si:H exhibits exceptional optoelectronic properties, enabling it to accommodate atoms of various sizes and form alloys with elements like germanium and carbon. The gap of this material can be precisely controlled by adjusting the compositions of

Chapter one: generality about solar cells

gas mixtures during manufacturing. Consequently, a-Si:H solar cells have the potential to emerge as significant competitors to conventional electricity sources.

However, there are certain limitations associated with a-Si:H. These include an increased density of dangling bonds per alloy, degradation of optoelectronic properties when exposed to prolonged solar irradiation, and a disparity between the material's absorption characteristics and the solar spectrum

1.10.1.2-Doping of hydrogenated amorphous silicon

Amorphous silicon, first prepared in the mid-1960s through thermal evaporation and spraying, was found to be strongly defective and unsuitable for cell applications. Chittick's work in 1969 demonstrated that Mott's rule on the insensitivity of semiconductor doping in amorphous silicon cannot be strictly obeyed. However, amorphous silicon prepared by "glow discharge" reduced its defect density, leading to the discovery of amorphous silicon hydrogenated (a-Si:H). Spear's group in 1975 demonstrated that the "glow discharge" of a-Si:H can be prepared with a low defect concentration, allowing for the movement of the Fermi level in the gap. Carlson and Wronski predicted that doping is possible only when the defect density < defect density doping, leading to the manufacture of the first a-Si:H solar cells with an efficiency of 2 to 2.5%. [11]

1.10.1.3-Hydrogenated amorphous Silicon-Germanium alloy

Hydrogenated amorphous Silicon Germanium (a-SiGe:H) was first deposited by Chittick et al. through glow-discharge of silane and germane gas. Chevallier et al. demonstrated that the optical gap of this material can be changed from 1.7 eV (a-Si:H) to 1.1 eV (a-SiGe:H) by changing the alloy's composition. This led Marfaring et al. to propose using a-SiGe:H alloys as a low gap partner of an a-Si/a-SiGe tandem cell for better absorption of longer wavelengths of the solar spectrum. CVD, PECVD, RF, and microwave CVD techniques have been used to prepare layered quality devices.

However, the properties of a-SiGe:H films deteriorate rapidly with increasing reduction of the optical gap, resulting in increased incorporation of Ge. Traditional deposition settings for based devices a-Si:H could not produce high-quality a-SiGe:H material in this range of compositions. Highly photoconductive a-SiGe:H films with very low densities defects were

Chapter one: generality about solar cells

produced by the deposition technique (PECVD) with low flow rate source gases and hydrogen dilution

1.10.2-Single and multijunction solar cells based on amorphous silicon hydrogen

1.10.2.1-Single junction solar cells

1.10.2.1.1-Structure of a-Si-based solar cells

A crystalline solar cell consists of a p-type domain and a p-type domain, which form a PN junction to separate photo-generated electron-hole pairs and prevent recombination. In amorphous and microcrystalline silicon solar cells, diffusion lengths are short due to the mobility of carriers and short lifespans. In doped a-Si:H, diffusion lengths are even shorter due to higher concentration of defects. To ensure photovoltaic activity, an intrinsic layer with low defect density must be incorporated between the p-type and n-type layers. This layer allows for the free path average of the slowest carriers to separate them in electron space. However, the presence of a free field in any appreciable length of the layer drastically reduces collection yield. The electric field is higher near the p+ contacts and n+ contacts, but the field is reduced near the maximum power point, resulting in a virtual free field region in the center of layer i. These p+ structures are typically called solar cell type drift, unlike crystalline solar cells where photocurrent is independent of external voltage

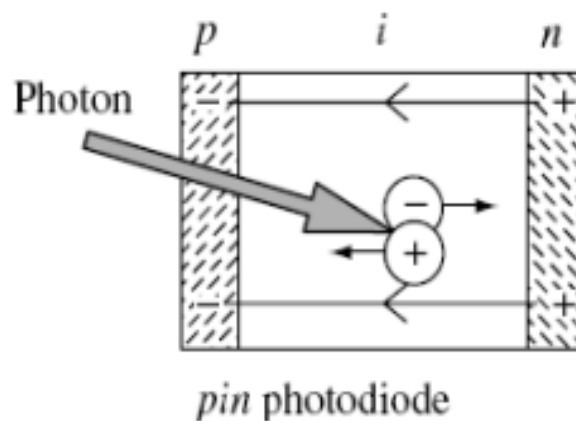


Figure1.13:cell solar of pin photodiode[11]

1.10.2.2-Multijunction solar cells

1.10.2.2.1- Multijunction solar cells based on a-Si:H

Chapter one: generality about solar cells

Multi-junction solar cells offer advanced technology to enhance the efficiency of converting solar energy into electrical energy. Compared to solar cells with a simple p-i-n junction structure, multi-junction cells can achieve significant performance improvements.

a-Working principle

Multijunction solar cells are based on the principle of stacking multiple layers of p-i-n structures with different optical gaps. These layers are designed to better absorb specific wavelengths of sunlight, allowing the sun's energy to be harnessed more efficiently.

b-Advantages of multi-junction solar cells

- More efficient use of solar spectrum: Each layer is designed to absorb a specific band of the spectrum, reducing wasted light energy.
- Optimized carrier collection: Multi-junction architecture reduces charge carrier recombination, improving current collection efficiency.
- Reduced light-induced degradation: Multi-junction structure reduces the effect of light-induced degradation, extending the life of the solar cell.
- Multi-junction solar cells achieve a much higher stable yield compared to single-junction solar cells, even if the additional cells have the same gap as the first cell.

c-Types of multi-junction solar cells

Duplex: It is made of two layers of p-i-n with different optical gaps.

Triple junction: It is made of three layers of p-i-n with different optical gaps.

Multijunction: Made of four or more layers of p-i-n with different optical gaps.

1.11-Conclusion

In this chapter, we give a general overview of solar cells and its different generation. We also presented a general overview of amorphous silicon and its alloys which are studied in this work.



**Chapter tow: presentation
of the simulation software**

Chapter tow: presentation of the simulation software

2.1-Introduction

In this chapter, we will introduce the AFORS-Het software and how to use it. This software includes a wide range of integrated studies functions, where it performs numerical simulation of cells and solar measurements.

2.2-Simulation

2.2.1-Definition

Simulation is the process of creating a computer program or model that simulates or replicates scenarios or operations in the real world. The purpose of simulation is to test hypotheses, predict outcomes, or evaluate the effects of changes in a controlled environment. It is commonly used in fields such as science, engineering, economics, and social sciences.

Simulation involves creating a mathematical or logical model of a system or process and running it on a computer. The model relies on physical laws or statistical data, or both, and the simulation program generates results based on the inputs and assumptions made in the model. Overall, simulation is a powerful tool for understanding and analyzing complex systems and processes in a safe and controlled environment.

2.2.2-Basic concepts in cell simulation

Electron Affinity: As previously explained, it's the amount of energy released when an electron is added to a neutral atom to form a negative ion.

Band Gap: In solid-state physics, it's the energy difference between the top of the valence band and the bottom of the conduction band in insulators and semiconductors. It determines the electrical conductivity of the material.

Optical Band Gap: Similar to the regular band gap, but specifically referring to the energy range over which a material does not absorb light. It's important in determining a material's optical properties, such as transparency and color.

Effective Conduction Band Density: This refers to the effective density of states (number of available energy states) in the conduction band of a semiconductor. It influences the electrical conductivity of the material.

Chapter tow: presentation of the simulation software

Effective Valence Band Density: Similar to the conduction band density, but for the valence band. It affects the behavior of holes (missing electrons) in the material.

Effective Electron Mobility: It describes how easily electrons can move through a material when subjected to an electric field. Higher electron mobility leads to better conductivity.

Effective Hole Mobility: Similar to electron mobility, but for holes. It measures how easily holes can move

Doping Concentration Donors: It refers to the number of donor atoms added to a semiconductor lattice, which provide the lattice with free electrons. Donor impurities contribute to increasing the conductivity of the semiconductor material, as the free electrons can move easily through the lattice.

Doping Concentration Acceptors: It refers to the number of acceptor atoms added to a semiconductor lattice, which accept free electrons. Acceptor impurities create holes in the lattice, allowing electrons in the lattice to move to fill these holes

Electron thermal velocity: is the average velocity of electrons due to their thermal energy.

Hole thermal velocity: is the average velocity of "holes" in a semiconductor lattice due to their thermal energy. Holes behave like positively charged particles in the absence of an electron.

Layer density: could refer to the density of atoms or molecules in a particular layer of a semiconductor material.

2.2.2- Equivalent diagram of a solar cell

A. Case of an ideal solar cell

The solar cell is said to be ideal if the current-voltage relationship is given by the following expression:[4]

$$I=I_{ph}-I_s [e^{qv/nkT}-1] \quad (2.1)$$

Chapter tow: presentation of the simulation software

I_{ph} : optical current

k : Boltzmann constant $k= 1.38 \times 10^{-23}$ j/k

\hat{q} : The charge of the electron is $q=1.602 \times 10^{-19}$ C

T : absolute temperature of the cell

The solar cell under illumination can be schematized by a current generator I_{ph} (an inverse current proportional to incident light) in parallel with a diode delivering a current

$$I_d = I_s [e^{qv/nkT} - 1] \quad (2.2)$$

We thus obtain the equivalent circuit of an ideal solar cell, presented on the following figure

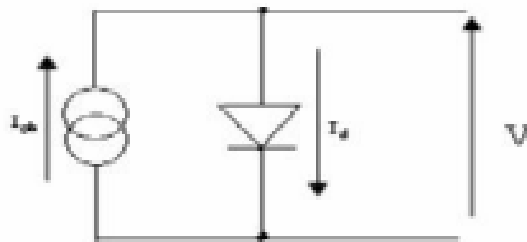


Figure 2.1: equivalent diagram of the ideal solar cell

B. Case of a real solar cell

The equivalent diagram of the real photovoltaic cell takes into account two resistances; a series resistance R_s representing the various contact resistances and of connections, and a resistor R_{sh} (shunt) in parallel with the current generator which characterizes the various leakage currents due to the diode.

If V is the voltage across the diode, the characteristic equation of the real cell is then given by:[4]

$$I_d = I_s [e^{q(v+IR_s)/nkT} - 1] \quad (2.3)$$

Chapter tow: presentation of the simulation software

$$I_{ph} = I + I_d + I_{sh} \quad (2.4)$$

$$I_{sh} = (V + IR_s) / R_{sh} \quad (2.5)$$

$$I = I_{ph} - I_s [e^{q(v+IR_s)/nkT} - 1] - (V + IR_s) / R_{sh} \quad (2.6)$$

$$\text{We pose: } R_{sh} = 1/G_p \quad (2.7)$$

So the equation becomes:

$$I = I_{ph} - I_s [e^{q(v+IR_s)/nkT} - 1] - G_p (V + IR_s) \quad (2.8)$$

With:

I_{ph} Photo generation current density.

G_p are the generation rates of electrons and holes

R_s Electron charge

R_{sh} Thermodynamic potential.

q Diffusion potential.

The equivalent diagram of the solar cell is the model shown in the following figure

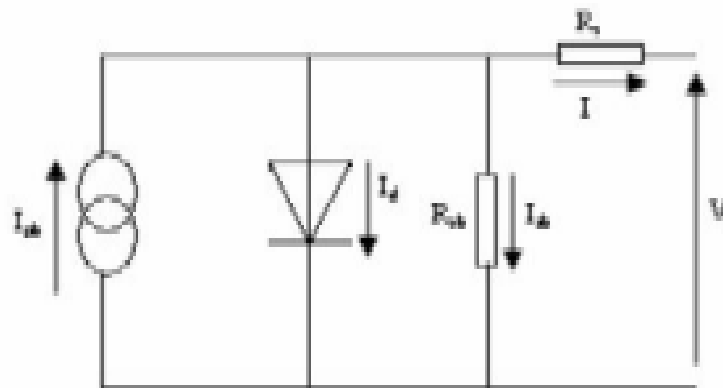


Figure 2.2: Equivalent diagram of the solar cell

2.2.3-Electrical Characteristics of the Solar Cell

a- Open-Circuit Voltage (Voc)

The open-circuit voltage is the voltage difference between the terminals of the device when the circuit is open, meaning there is no electrical load, and therefore no current flows through the circuit. [4]

$$V_{oc} = \frac{nkT}{q} \ln\left(\frac{I_{ph}}{I} + 1\right) \quad (2.9)$$

With: k is the Boltzmann constant, q is the electric charge, T is the temperature absolute, n is the ideality factor.

b- Short-Circuit Current (Isc)

It is an extremely high current that suddenly flows through a circuit that cannot withstand it, causing the weakest point in the circuit to open. The reason for the passage of this very high current is due to the contact of two cables (wires) with a voltage difference and very low resistance between them (short circuit). According to Ohm's law, the current flowing through the cable will be extremely high, and this is the short-circuit current. [4]

$$I_{sc} = \frac{I_{ph}}{1 + \frac{R_s}{R_{sh}}} \quad (2.10)$$

c- Maximum Power Point (Pmax)

It is the operating point at which the solar cell yields the maximum possible power output. The maximum power of the cell is practically measured under standard test conditions (STC), which include an irradiance of 1000 W/m² and a temperature of 25°C. [4]

$$P_m = I_m \times V_m \quad (2.11)$$

d- Fill Factor (FF)

It is a coefficient that reflects the quality of the solar cell, representing the ratio between the maximum power (Pmax) and the ideal power. [4]

$$FF = \frac{I_m \times V_m}{V_{oc} \times I_{sc}} = \frac{P_m}{V_{oc} \times I_{sc}} \quad (2.12)$$

e- Solar Cell Efficiency (η)

Defined as the ratio between the maximum power output of the cell and the solar irradiance reaching the cell. [4]

$$\eta = \frac{P_m}{P_{in}} \quad (2.13)$$

2.2.4-The Current-Voltage (IV) characteristic curve :

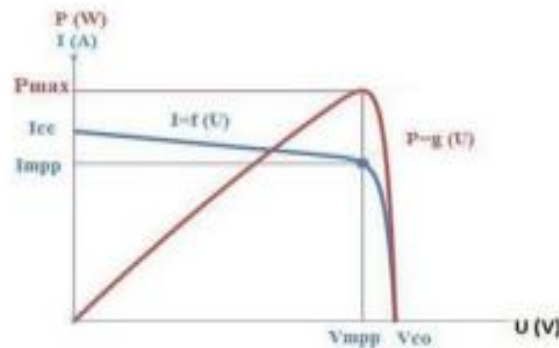


Figure 2.3: represents the characteristic Current-Voltage (IV) curves for a solar cell in both under darkness and light exposure. [1]

-The red curve represents the Power-Voltage (P-V) curve.

-The blue curve represents the Current-Voltage (I-V) curve.

2.3-The electric model

In the electrical model, three associated differential equations: the equation of Poisson and the two charge carrier continuity equations are solved simultaneously in the state of equilibrium and out of thermodynamic equilibrium (i.e. under the effect bias voltage or light, or both). [4]

The equations used are:

Poisson's equation

$$\frac{\partial^2 \varphi(x)}{\partial x^2} = \rho(x)/\varepsilon \quad (2.14)$$

ε : represents the dielectric constant.

$\varphi(x)$: the electrostatic potential

x : the position in the device.

The continuity equation for holes

$$G(x) - R(p(x).n(x)) - \left(\frac{1}{q}\right)\left(\frac{\partial J_p(x)}{\partial x}\right) = 0 \quad (2.15)$$

With: p and n : the densities of the holes and electrons in the valence and conduction bands,

q : the electronic charge,

R : the recombination rate, G : the rate of generation of electron-hole pairs,

J_p : the current densities of the holes respectively.

The electron continuity equation

$$G(x) - R(p(x).n(x)) - \left(\frac{1}{q}\right)\left(\frac{\partial J_n(x)}{\partial x}\right) = 0 \quad (2.16)$$

J_n : the current densities of the electrons

The charge density is given by

$$\rho(x) = q ([p(x) - n(x) + p_T(x) - n_T(x) + N_{net}^+]) \quad (2.17)$$

With: p_T and n_T the density of trapped holes and electrons respectively,

N_{net}^+ : the effective doping density.

The electric field

$$E = \frac{\partial \phi(x)}{\partial x} \quad (2.18)$$

With: E: The electric field

2.4-Simulation software

2.4.1-An overview of the AFORS-Het software

AFORS-Het is a computer software specialized in the design and simulation of semiconductor systems and electronic devices. It is among the common modelling tools used in electronic and microelectronic industries. The program is distinguished by its ability to analyse various electrical and optical properties of semiconductor devices, such as diodes, transistors, as well as optical devices like LEDs and OLEDs.

AFORS-HET provides an advanced simulation environment that allows users to analyse many different aspects of semiconductor devices, including electrical properties such as current, voltage, and resistance, and optical properties such as emission and absorption. The software relies on advanced modelling and accurate digital calculations to provide precise and reliable results.

The software is typically used in academic research and industrial applications, where it helps engineers and researchers better understand the behaviour of semiconductor devices and improve their designs before manufacturing and using them in practical applications.

It is a software package used to simulate the performance of solar cells. It is specifically designed to model the behavior of non-homogeneous solar cells, which are a type of solar cells that combine different materials with different bandgaps to improve cell efficiency.

It includes a one-dimensional digital computer program for modeling multi-layered solar cells, whether homogeneous or non-homogeneous, as well as some common cell description methods. Solar cells, in terms of simulation, are divided into two sections:

Optical simulation: In this simulation, the local generation rate (G) is calculated inside the solar cell, which represents the number of excess carriers (electrons and holes) generated per

Chapter two: presentation of the simulation software

second and per unit volume at time t and position x within the solar cell due to light absorption. [1]

Electrical simulation: It calculates the local electron and hole densities (n) and the local electrical charge (P) within the solar cell. [1]



Figure 2.4: AFORS-HET program icon

2.4.2-Simulating the structure of a solar cell using the AFORS-Het software

AFORS-Het features an intuitive graphical interface that allows easy definition of structures (layer assembly) while controlling most physical parameters (electron affinity, band gap energy, mobility, doping, etc.). This interface is basically divided into three areas, as shown in Figure 2.5:

First zone: control program

This is where the structure to be simulated can be defined, as well as the parameters of the material being used. In a structure, one can find: a front contact, back contact, and a certain number of layers between which interfaces exist.

Second zone: external parameters

Chapter two: presentation of the simulation software

External parameters are divided into three groups: external temperature, illumination spectrum, and boundary conditions.

Third zone: measurements

This is where one can choose the measurement to be performed.

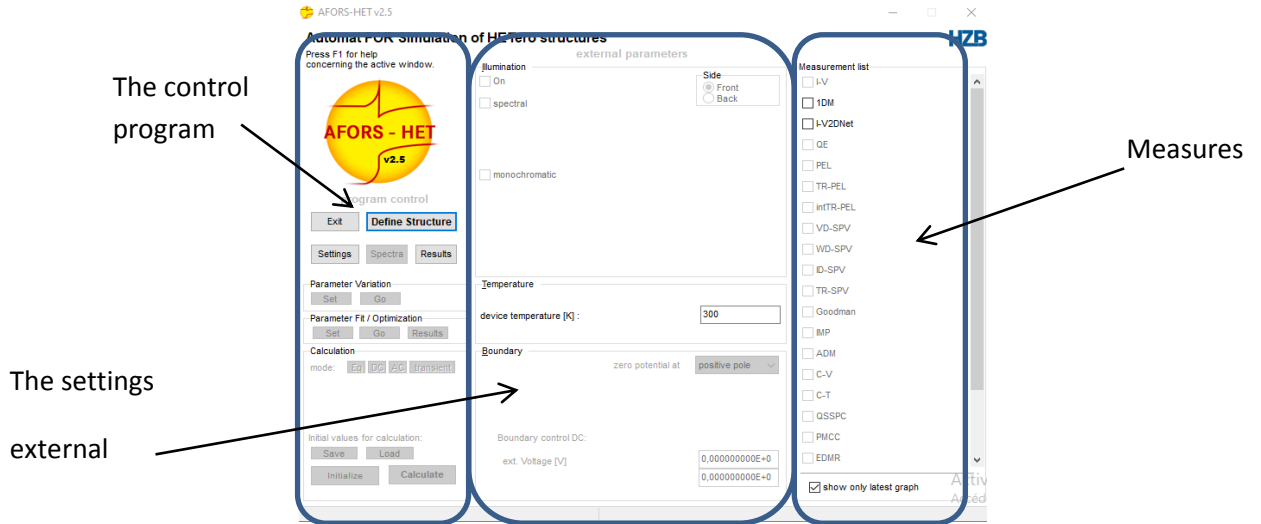
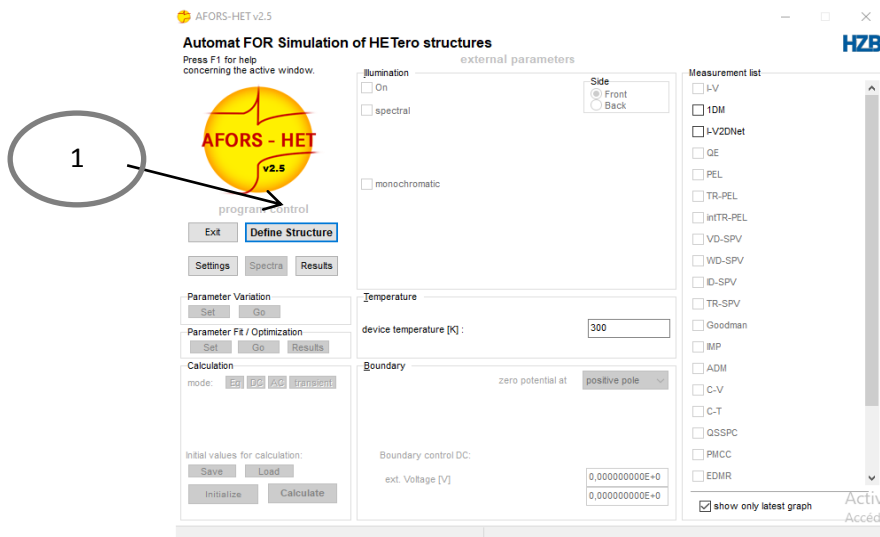


Figure 2.5: Graphical interface of the 1D simulation software AFORS-HET.

To explain how this program works, we follow these steps:

Once the program is opened, the window appears (figure 2.6).



The figure 2.6: define structure of the solar cell.

This window, Figure (2.6), contains:

Instruction number1: Define structure

This instruction allows us to design the structure of the solar cell we want to study. When this instruction is clicked, a window appears, as shown in Figure 2.7.

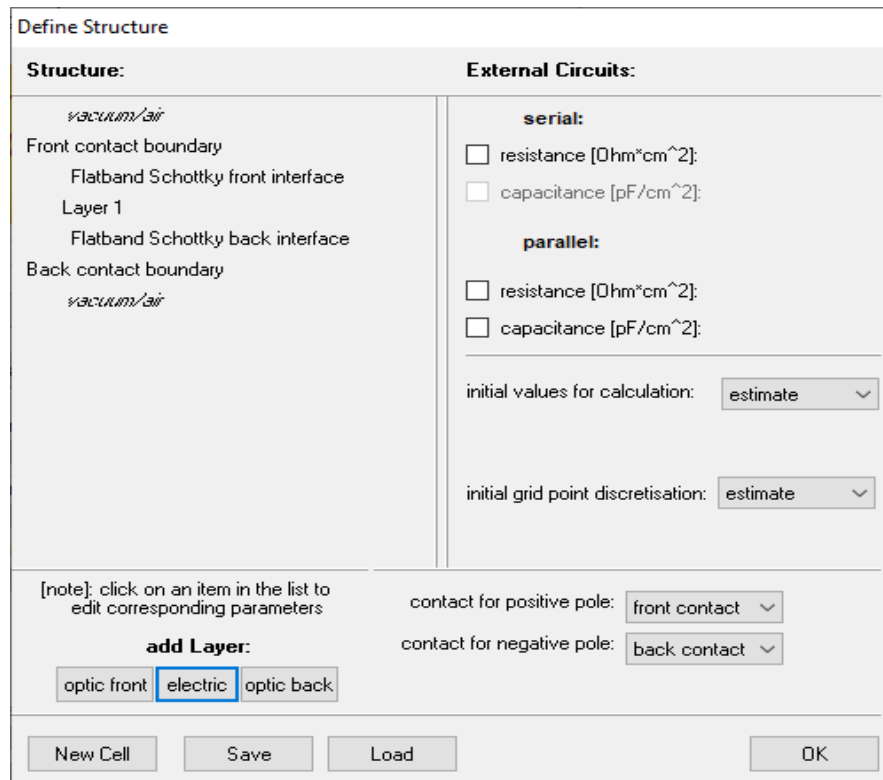


Figure 2.7: Window of the structure of the solar cell.

To define the layers:

1. On the left side of the window, click on "1 Layer" to define the properties of the first layer composing the solar cell under study. To define the properties of the first layer, we have two cases:

a. If the first layer is available in the program's database, click on the "Load" instruction.

b. If the "1st Layer" is not available in the program's database, follow these steps:

- Click on "1 Layer" to display the "1 Layer" window, which shows the properties of the standard layer (figure 2.8).

- Modify these properties according to the studied layer (adjust the name, thickness, and other properties).

Chapter two: presentation of the simulation software

- Click on "OK".

Layer 1

name: Layer 1 [Load] [Save] [Delete]

bulk model: standard [specify] thickness [cm]: 0,015

electrical properties

functional dependance: Constant

dk [-]:	11.9
chi [eV]:	4.05
Eg [eV]:	1.124
Eg opt. [eV]:	1.124
Nc [cm ⁻³]:	2.846E19
Nv [cm ⁻³]:	2.695E19
μ [cm ² /Vs]:	1107
μp [cm ² /Vs]:	424.6
Na [cm ⁻³]:	0
Nd [cm ⁻³]:	2E15
ve [cm/s]:	1E07
vh [cm/s]:	1E07
ρ [g*cm ⁻³]:	2.328
rae [cm ⁶ /s]:	0
rah [cm ⁶ /s]:	0
rbb [cm ³ /s]:	0

FTM on F0 [V/cm] 2E05

defect properties

no defects [add] [edit] [delete]

layer properties

Taur [] s Lp [] cm

Taup [] s Ln [] cm

OK

optical properties

nk-File cSi.nk

constant nk:

α = 4 * π * k / λ

incoherent

Figure 2.8: introduction of the layer parameters

Note:

- To save the properties of the "1 Layer", click on the "Save" instruction and save this layer in a file.

- To delete the "1 Layer" from the structure, click on "Delete".

In Figure 2.7, note the instruction (2) "electric". Click on it to add the second layer to the solar cell. We can follow the same step as the first layer in order to change the parameters of the second layer.

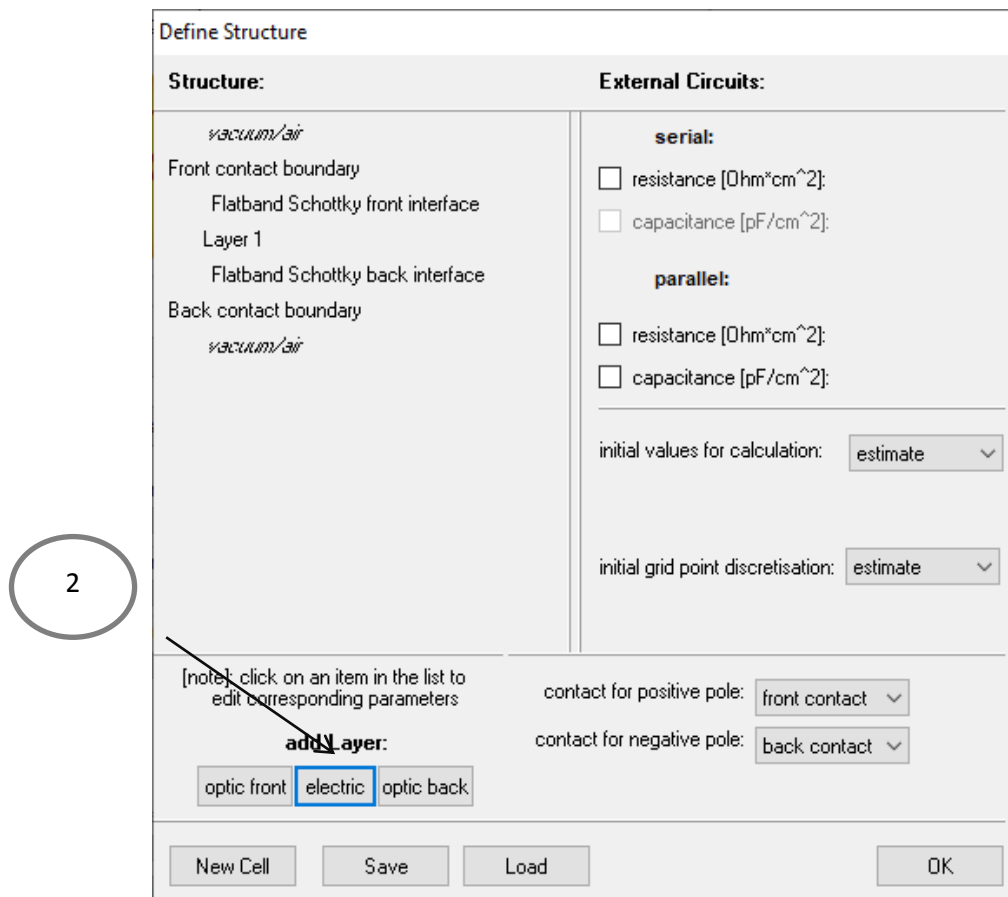


Figure 2.9: Adding a layer

Note:

- To load a previously saved cell structure, click on the "Load" instruction located at the bottom of the Define Structure window.
- To save the entire cell structure, click on the "Save" instruction located at the bottom of the Define Structure window.
- To add a new cell, click on the "Cell New" instruction located at the bottom of the Define Structure window.

Once all steps are completed, click "OK".

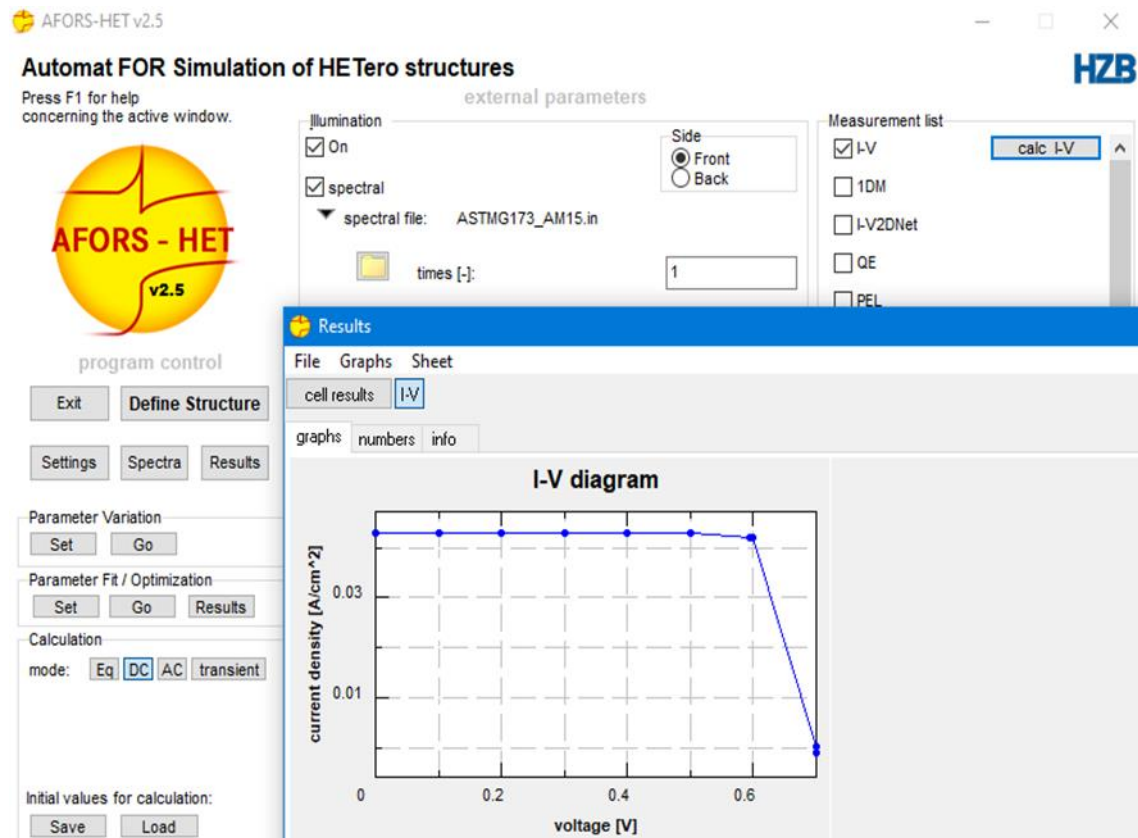


Figure 2.10 : I-V characteristic and illumination

We return to the first window, Figure 2.6, which allows us to choose the type of simulation:

A. Dark simulation: No illumination is present.

B. Illuminated simulation: We can select the type of radiation to study (Solar radiation Spectral or Monochromatic radiation). Before clicking "On", we choose the Direct Current (DC), then select the temperature, and afterwards choose the type of calculation from the measurement list that we want to compute. The characterisation I-V und illumination allow us to calculate the parameter of the solar cell which are the open voltage circuit V_{OC} , short current circuit J_{SC} , the fill factor FF and the efficiency, η (figure 2.10).

2.5- Conclusion

In this chapter, we provided a detailed description of the AFORS-HET program. We outlined its program structures, tools, and capabilities to retrieve all internal and external information related to the studied device (solar cell).



**Chapter Three: Results and
discussion**

3.1-Introduction

In this chapter, we expose the study of the hydrogenated amorphous silicon (a-Si:H) based cell. We start from the study of the effect of changing the parameters of a single Si. After that, we illustrate the effect of the variation of the parameters of SiGe solar cells. Finally, The study of the tandem Si and SiGe solar cells. For that, we discuss the software components and physical constants used in each layer. We will also discuss the results of the simulation carried out with the AFORS-Het program.

3.2-Results and discussion

3.2.1- The solar cell's particular structure of a-Si:H material

The solar cell under investigation in this study is composed of three layers. As shown in the figure 3.1, a-Si:H type n makes up the first layer, a-Si:H type i makes up the second layer, and a-Si:H type p makes up the last layer. The sun light enters into this cell from the top layer (type p). The solar cell under investigation, is with serial resistance $R=0.01 \Omega.cm^{-2}$ and parallel resistance $R_p=1e5 \Omega.cm^{-2}$, at a temperature of $T=300 K$.

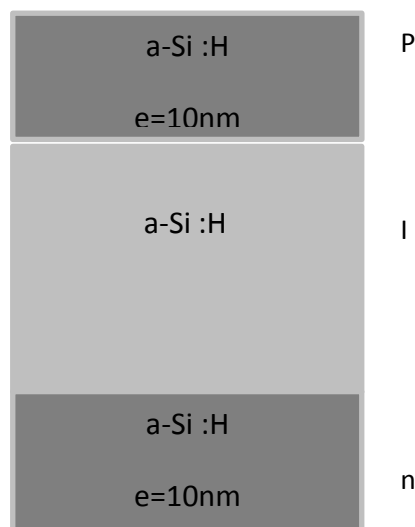


figure 3.1: Solar cell structure

3.2.2-Physical constants associated with each layer of the a-Si:H cell

This table provides information about the different parameters that affect the structure of the modeled cell. It can be used to understand the differences between various cells and identify the factors influencing cell design.

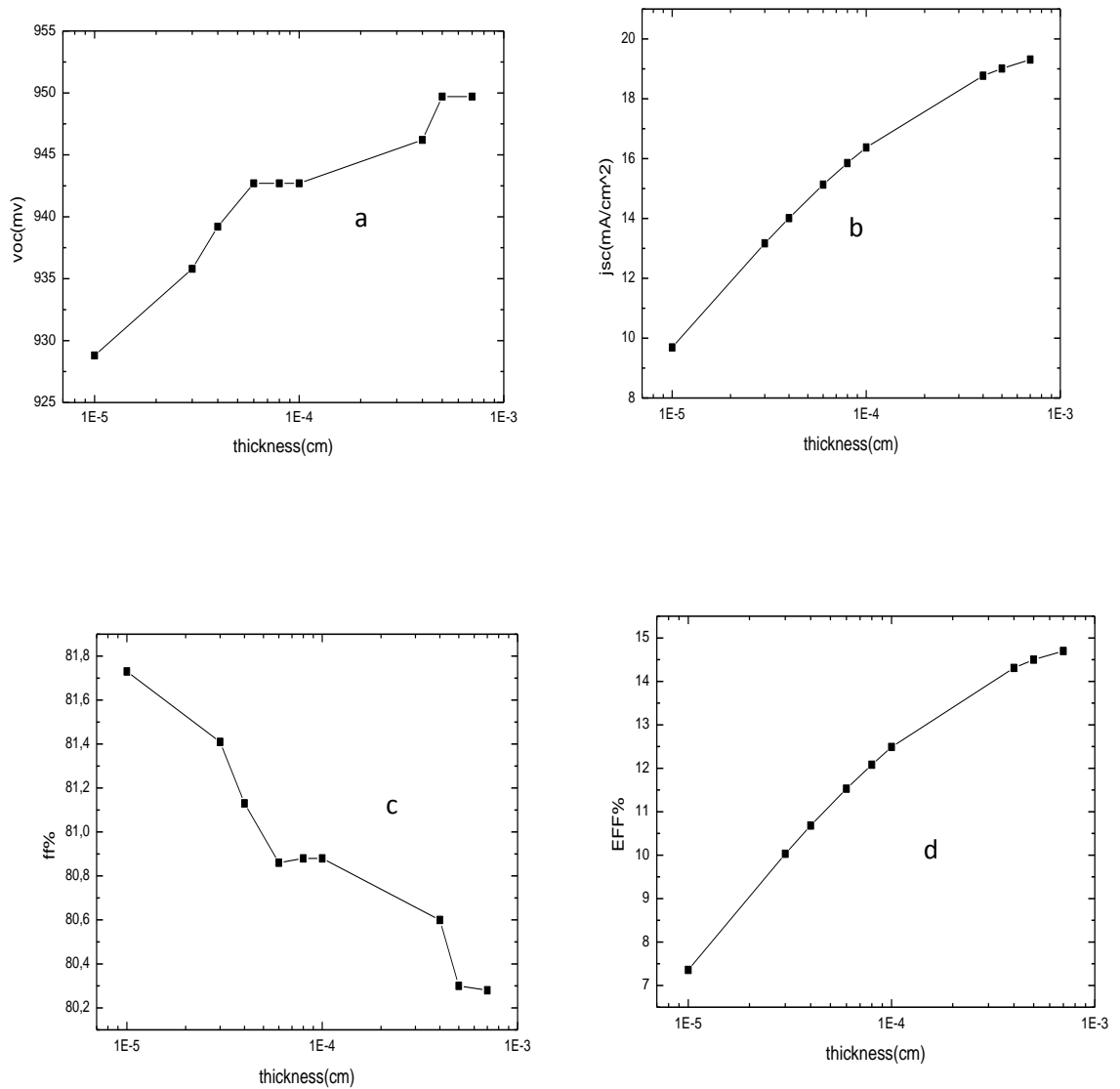
Chapter three: results and discussion

Table3.1 : Cell-simulating physical constants[12]

	a-Si:H (n)	a-Si:H (i)	a-Si:H (p)
Dk[-]	11.9	11.9	11.9
Chi [eV]	3.9	3.9	3.9
Eg [eV]	1.52	1.52	1.52
Eg opt[eV]	1.72	1.72	1.72
Nc [cm ⁻³]	2.846x10 ¹⁹	1x10 ²⁰	1x10 ²⁰
Nv[cm ⁻³]	2.685 x10 ¹⁹	1x10 ²⁰	1x10 ²⁰
μn[cm ² /Vs]	20	20	20
μp[cm ² /Vs]	5	5	5
Na[cm ⁻³]	0	0	1x10 ¹⁹
Nd [cm ⁻³]	1x10 ¹⁹	1000	0
Ve[cm/s]	1x10 ⁰⁶	1x10 ⁰⁶	1x10 ⁰⁶
Vh[cm/s]	5x10 ⁰⁶	1x10 ⁰⁶	5x10 ⁰⁶
Rho[g*cm ⁻³]	2.328	2.328	2.328

3.2.3- The effect of the thickness of the absorber layer on the cell properties

In this section, we will examine how the absorber layer's thickness affects the characteristics of the cell, which are denoted by the following: efficiency η , fill factor FF, open circuit voltage V_{oc} , and short circuit current J_{sc} . The figure 3.1 shows the evolution of these parameters as a function of the thickness of the absorber layer.



Chapter three: results and discussion

Figure 3.2: the evolution of the open circuit voltage V_{oc} (a), the short circuit current J_{sc} (b), the fill factor FF (c) and the efficiency η (d) as a function of the thickness of the absorber layer.

Open circuit voltage V_{oc} :

From the figure 3.2, we can notice, that there is a significant relationship between open circuit voltage values and the thickness of the a-Si:H type i layer. We notice an increase in the open circuit voltage values from 928,8 mV to 949,7 mV when the thickness increases from 0.1 μm to 7 μm .

Short circuit current J_{sc} :

Also, we notice that there is an increase of the short circuit current values from 9,7 to 19,3 mA/cm^2 when the thickness increases from 0.1 μm to 7 μm .

Fill factor FF :

For the fill factor we can observe a decrease of this parameter from 81,7% to 80,27% when the layer's thickness increases from 0.1 μm to 7 μm .

Efficiency η :

Finally, from the curve d there is an increase of the efficiency η from 7,3% to 14,7% when the thickness increases from 0.1 μm to 7 μm .

3.2.4- The solar cell's particular structure of a-SiGe:H material

The solar cell under investigation in this study is composed of three layers.

As shown in the figure 3.3, a-SiGe:H type n makes up the first layer, a-SiGe:H type i makes up the second layer, and a-SiGe:H type p makes up the last layer. The sun light enters into this cell from the top layer (type p). The solar cell under investigation, is with serial resistance $R=0.01 \Omega.\text{cm}^{-2}$ and parallel resistance $R_p=1 \times 10^5 \Omega.\text{cm}^{-2}$, temperature of $T=300 \text{ K}$

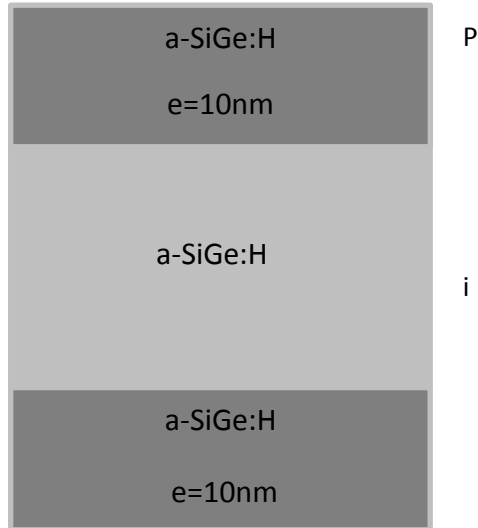


figure 3.3: Solar cell structure of a-SiGe:H

3.2.5-Physical constants associated with each layer of the a-SiGe:H cell

Table 3.2: Cell-simulating physical constants [13]

	a-SiGe:H (n)	a-SiGe:H (i)	a-SiGe:H (p)
Dk[-]	11.9	11.9	11.9
Chi[eV]	4.17	4.17	4.17
Eg[eV]	1.5	1.5	1.5
Eg opt[eV]	1.5	1.5	1.5
Nc[cm ⁻³]	2.5×10^{20}	2.5×10^{20}	2.5×10^{20}
Nv[cm ⁻³]	2.5×10^{20}	2.5×10^{20}	2.5×10^{20}

Chapter three: results and discussion

$\mu_n[\text{cm}^2/\text{Vs}]$	10	10	10
$\mu_p[\text{cm}^2/\text{Vs}]$	2	2	2
$N_a[\text{cm}^{-3}]$	0	0	1×10^{19}
$N_d[\text{cm}^{-3}]$	1×10^{19}	1000	0
$V_e [\text{cm/s}]$	1×10^{06}	1×10^{06}	1×10^{06}
$V_h[\text{cm/s}]$	5×10^{06}	1×10^{06}	5×10^{06}
$\text{Rho} [\text{g} \cdot \text{cm}^{-3}]$	2.328	2.328	2.328

3.2.6-The effect of the thickness of the absorber layer on the cell properties

In this section, we will examine how the absorber layer's thickness affects the characteristics of the cell, which are denoted by the following: efficiency η , fill factor FF, open circuit voltage V_{oc} , and short circuit current J_{sc} . The figure 3.4 shows the evolution these parameters as a function of the thickness of the absorber layer.

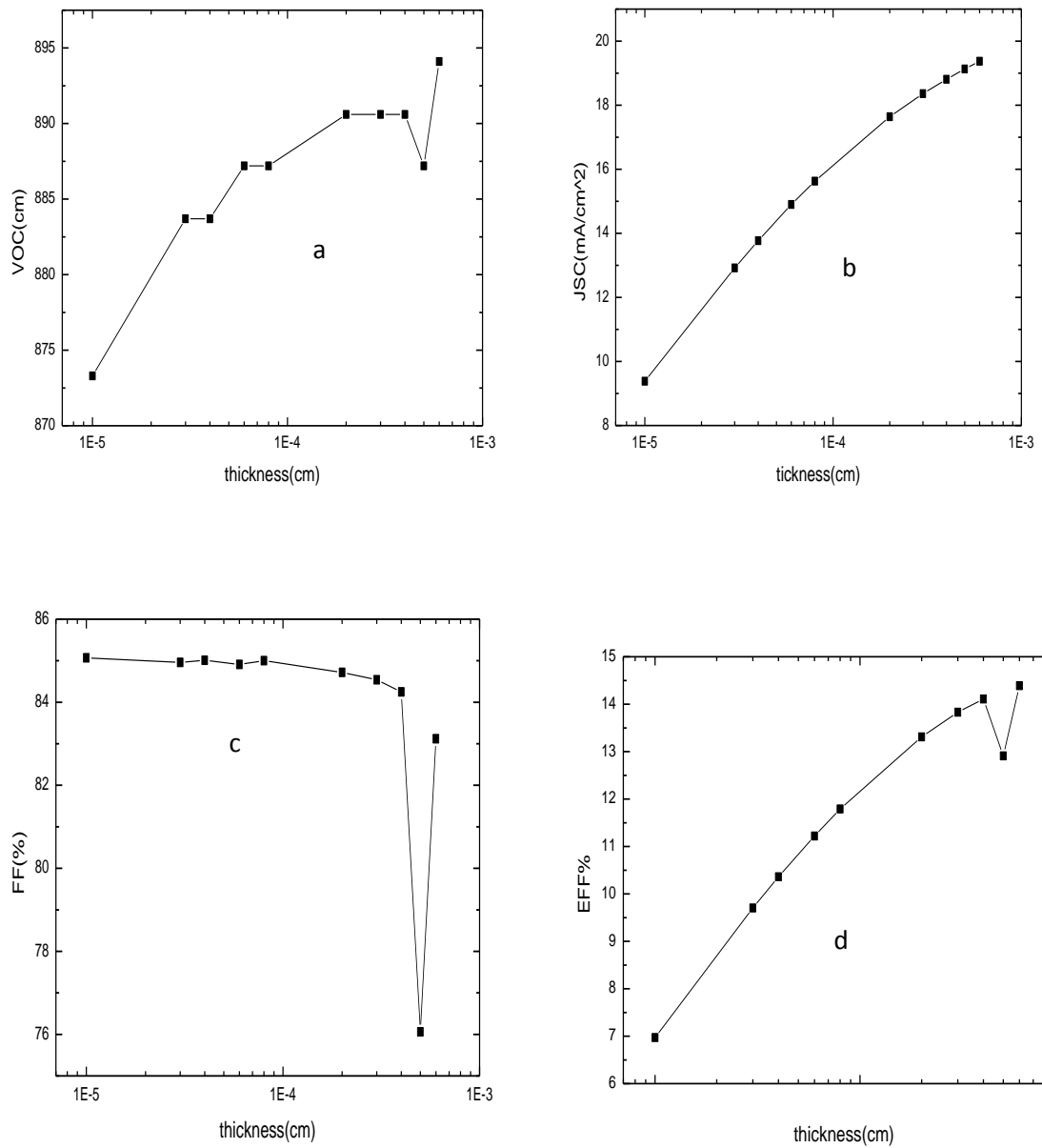


Figure 3.4: the evolution of the open circuit voltage V_{oc} (a), the short circuit current J_{sc} (b), the fill factor FF (c) and the efficiency η (d) as a function of the thickness of the absorber layer

Open circuit voltage V_{OC}

From the figure 3.4 in curve (a), we can observe that there is a significant relationship between the open circuit voltage values and the thickness of the i-type a-Si:H layer. We observe an increase in the open circuit voltage values from 873.3 mV to 887.2 mV when the thickness increases from 0.1 μm to 0.8 μm . The value was fixed at 890.6 mV when the thickness was increased from 2 μm to 4 μm and its value increased until 894.1 when the thickness increases to 6 μm .

Short circuit current J_{sc}

We also notice that there is an increase in the short circuit current values from 9.382 to 19.37 mA/cm^{-2} when the thickness increases from 0.1 to 7 μm

Filling factor FF

Regarding the filling factor, we note that this parameter decreases from 85.07 to 83.12% when the layer thickness increases from 0.1 to 7 μm

Efficiency η

Finally, from the curve d there is an increase in the efficiency η from 6.97 to 14.39 % when the thickness increases from 0.1 to 7 μm .

3.2.7- The special structure of tandem solar cell (a-Si:H, a-SiGe:H):

The solar cell under study in this study consists of four layers, As shown in Figure 3.5, a-Si:H n-type forms the first layer, a-Si:H i-type forms the second layer and a third layer of a-SiGe:H type i, forming Type a-Si:H p last layer. Sunlight enters this cell from the upper layer (p-type). The solar cell under study has a series resistance $R=0.01 \Omega.\text{cm}^2$ and a parallel resistance $R_p=1 \times 10^5 \Omega.\text{cm}^2$, at a temperature $T=300 \text{ K}$.

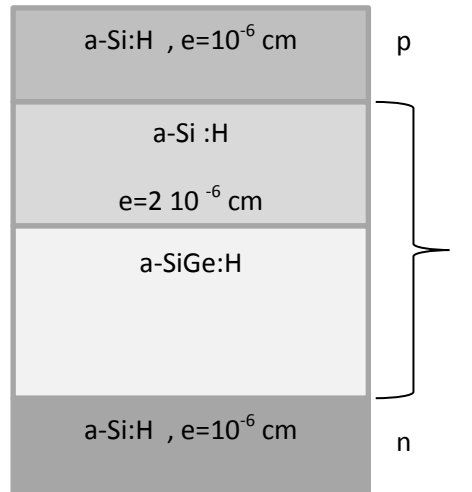


Figure 3.5: Structure of tandem solar cells (a-Si:H,a-SiGe:H)

3.2.8-Physical constants associated with each layer of the a-Si:H cell

Table3.3 : Cell-simulating physical constants[14]

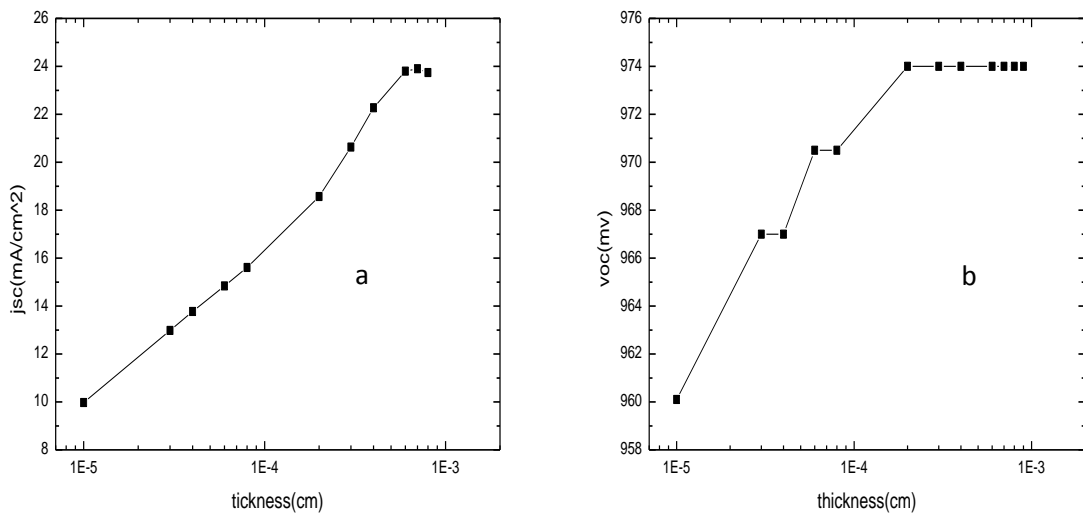
	a-Si:H (n)	a-Si:H (i)	a-SiGe:H (i)	a-Si:H(p)
Dk[-]	11.9	11.9	11.9	11.9
Chi[eV]	3.9	3.9	3.9	3.9
Eg[eV]	1.52	1.68	1.58	1.52
Eg opt[eV]	1.72	1.72	1.45	1.72
Nc[cm ⁻³]	2.846×10^{19}	4×10^{20}	4×10^{20}	1×10^{20}
Nv[cm ⁻³]	2.685×10^{19}	4×10^{20}	4×10^{20}	1×10^{20}
μ_n [cm ² /Vs]	20	1	2	20
μ_p [cm ² /Vs]	5	0.1	0.2	5
Na [cm ⁻³]	0	0	0	1×10^{19}
Nd [cm ⁻³]	1×10^{19}	1000	1000	0

Chapter three: results and discussion

Ve[cm/s]	1 x10 ⁰⁶	1 x10 ⁰⁶	1 x10 ⁰⁶	1 x10 ⁰⁶
Vh[cm/s]	5 x10 ⁰⁶	1 x10 ⁰⁶	1 x10 ⁰⁶	5 x10 ⁰⁶
Rho[g*cm ⁻³]	2.328	2.328	2.328	2.328

3.2.9- The effect of the thickness of the absorber layer on the cell properties

In this section, we will examine how the absorber layer's thickness affects the characteristics of the cell, which are denoted by the following: efficiency η , fill factor FF, open circuit voltage Voc, and short circuit current Jsc. The figure 3.6 shows the evolution of these parameters as a function of the thickness of the absorber layer.



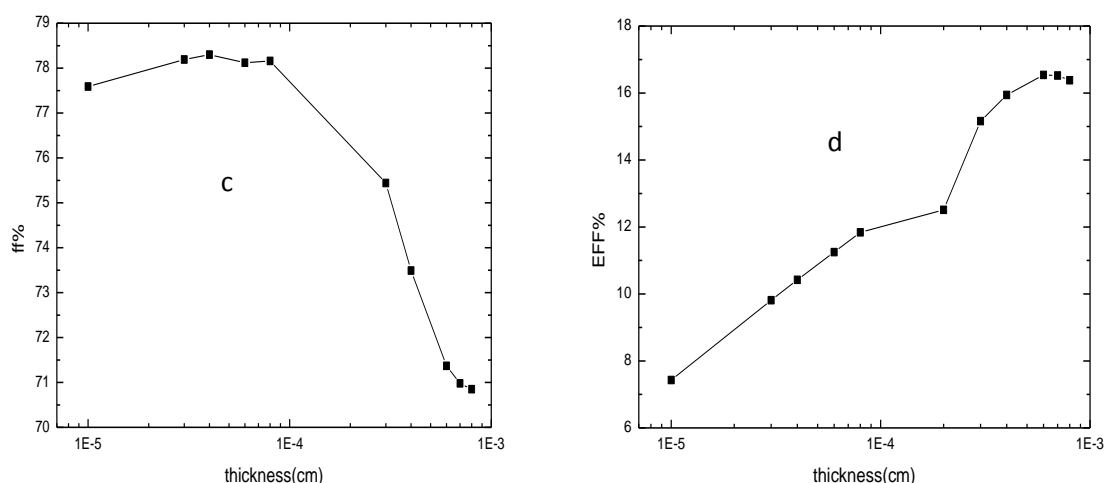


Figure 3.6: the evolution of the open circuit voltage V_{oc} (a), the short circuit current J_{sc} (b), the fill factor FF (c) and the efficiency η (d) as a function of the thickness of the absorber layer

Open circuit voltage VOC

From the figure 3.6. In curve a, we can observe that there is a significant relationship between the open circuit voltage values and the thickness of the i-type a-Si:H layer. We observe an increase in the open circuit voltage values from 960.1 mV to 970.5 mV when the thickness increases from 0.1 μm to 0.8 μm . We noticed that the value remained constant at 974 mV when the thickness increased from 2 μm to 7 μm .

Short circuit current JSC:

We also notice that there is an increase in short circuit current values from 9.971 to 23.9 mA/cm^2 when its thickness increases from 0.1 μm to 7 μm .

Filling factor FF:

Regarding the filling factor, we note that this parameter increases from 77.59 to 78.30% when the thickness of the layer increases from 0.1 μm to 0.4 μm . It decreases from 78.12 to 70.85% when the thickness increases from 0.6 μm to 8 μm .

Efficiency η :

Chapter three: results and discussion

Finally, from the curve d there is an increase in the efficiency η from 7.43 to 16.52% when the thickness increases from 0.1 μm to 7 μm .

-The increase in efficiency eff , open circuit voltage V_{oc} and short current J_{sc} with the increase of the absorption layer thickness in the solar cell is due to several reasons:

Increase in the amount of light absorbed: As the thickness of the absorbing layer increases, more photons are able to interact with the absorbing material, which leads to an increase in the amount of light absorbed and thus increased electricity production.

Increase in the number of charge carriers: The chance of generating charge carriers increases with the increase in the thickness of the absorbent layer, as more electron-hole pairs are produced in the absorbent layer. This leads to an increase in short-circuit current.

Increase in open circuit voltage: As the amount of light absorbed and the number of charge carriers increases, more voltage is generated in the solar cell due to greater interaction between the generated carriers. This leads to an increase in open circuit voltage.

Increase in carrier collection efficiency: As the thickness of the absorption layer increases, the carrier collection efficiency in the solar cell improves, which contributes to increasing the overall efficiency of the cell.

The fill factor decreases by several factors with the increase in the thickness of the absorber layer in the solar cell. We explain these factors as follow:

Increase in material losses: When the thickness of the absorbing layer increases, the number of electrical carriers that must be crossed to reach the collecting layers increases. This can increase material losses, as electrical carriers are susceptible to being blocked or obstructed when moving through the layer, reducing carrier collection efficiency and resulting in a decrease in fill factor.

Increase in internal resistance: Due to the increase in the thickness of the absorbing layer, the distance that the current must travel before reaching the collection point increases. This increases the internal resistance of the cell, which reduces the effectiveness of current transfer within the cell and thus reduces the fill factor

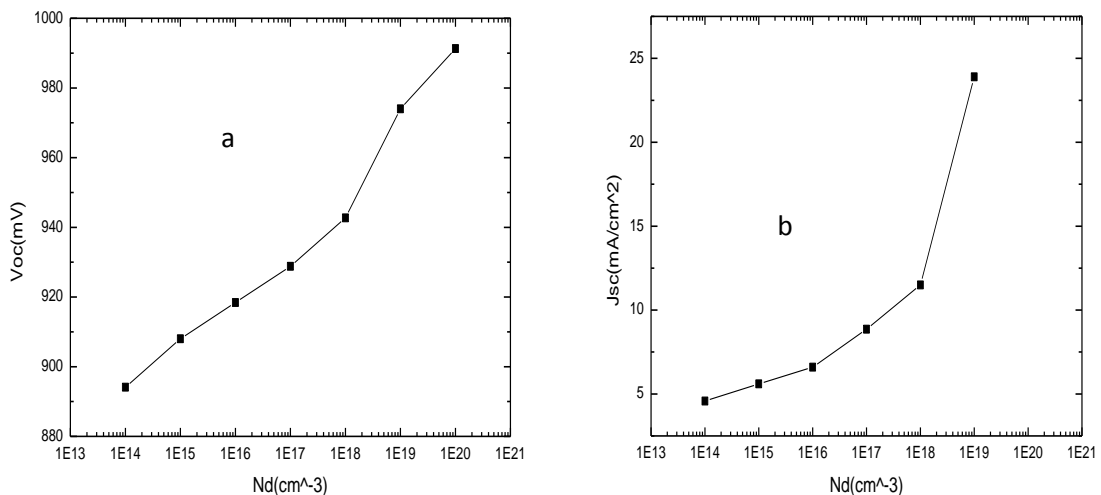
3.3 The effect of doping the a-Si:H(n) layer and a-Si:H(p) layer

In this part, we studied the effect of changing the concentration of donor N_D and acceptor N_A which are the doping of the n-type and p-type layers of the tandem solar cell, respectively. We varied N_A and N_D from $1 \times 10^{14} \text{ cm}^{-3}$ to $1 \times 10^{20} \text{ cm}^{-3}$

3.3.1-The effect of n-doping the a-Si:H(n) (the emitter) layer

In the figure 3.7 shows the evolution of the external parameters of our cell as a function of the concentration of the doping of the emitter. The doping concentration was varied from 1×10^{14} to $1 \times 10^{20} \text{ cm}^{-3}$.

From Figure 3.7, we observe the open circuit voltage V_{oc} increases from 894.1 to 991.1 mV as the doping increases from 1×10^{14} to $1 \times 10^{20} \text{ cm}^{-3}$. We record the highest value of $V_{oc} = 991.1 \text{ mV}$, and we also notice an increase in the current J_{sc} from 4.58 mA to 33.03 mA with an increase in the doping from 1×10^{14} to $1 \times 10^{20} \text{ cm}^{-3}$, while the FF increases from 51.71 % to 75.61% and the efficiency from 2.12 % To 24.76% when doping increases from 1×10^{14} to $1 \times 10^{20} \text{ cm}^{-3}$.



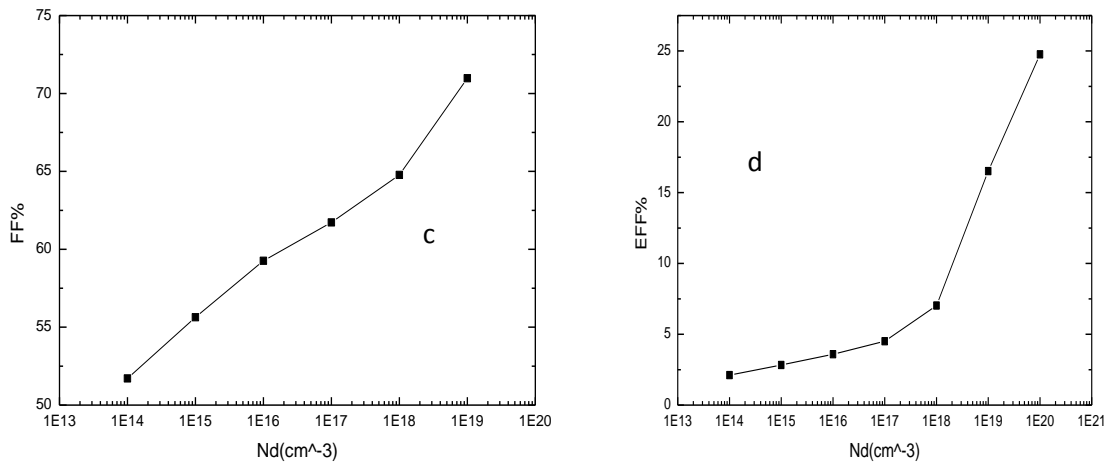


Figure 3.7: the evolution of the open circuit voltage V_{oc} (a), the short circuit current J_{sc} (b), the fill factor FF (c) and the efficiency η (d) as a function of of doping the a-Si:H(n) layer N_D in a tandem solar cell

Increasing the open-circuit voltage (V_{oc}), short-circuit current (J_{sc}), fill factor (FF), and efficiency by increasing doping in the n-layer can be explained as follows:

Improving the energy barrier: Increasing doping in the n-layer can lead to improving the energy barrier between the n-layer and the p-layer in the semiconductor, which increases the open-circuit voltage.

Enhancing carrier diffusion: Increasing doping can improve carrier diffusion within the n-layer, enhancing the fill factor and increasing the efficiency of the cell.

Overall, improving the doping level in the n-layer can lead to comprehensive improvements in the performance of solar cells, increasing their efficiency and ability to generate power.

3.3.2-The effect of p-doping of the a-Si:H(p) (the base) layer

In the figure 3.7 shows the evolution of the external parameters of our cell as a function of the concentration of the doping of the emitter. The doping concentration was varied from 1×10^{14} to $1 \times 10^{19} \text{ cm}^{-3}$.

From the figure 3.8, we observe an increasing of the open circuit voltage V_{oc} from 737.8 to 974mV with increasing of doping from 1×10^{14} to $1 \times 10^{19} \text{ cm}^{-3}$. Also, we observe an increase in J_{sc} from 23.42 mA to 23.90 mA with an increase in doping from $1 \times 10^{14} \text{ cm}^{-3}$ to $1 \times 10^{20} \text{ cm}^{-3}$, while we notice that FF decreases from 68.35% to 63.61%, then its value increases

Chapter three: results and discussion

to 76.51% at 1×10^{17} , then the value of FF decreases from 76.51% to 70.98% when the doping is increased from 1×10^{17} to $1 \times 10^{19} \text{ cm}^{-3}$. As for the efficiency, it increases from 11.81% to 16.52% when the doping is increased from 1×10^{14} to $1 \times 10^{19} \text{ cm}^{-3}$, it shows a maximum value of 16.52% at the doping concentration of $1 \times 10^{19} \text{ cm}^{-3}$.

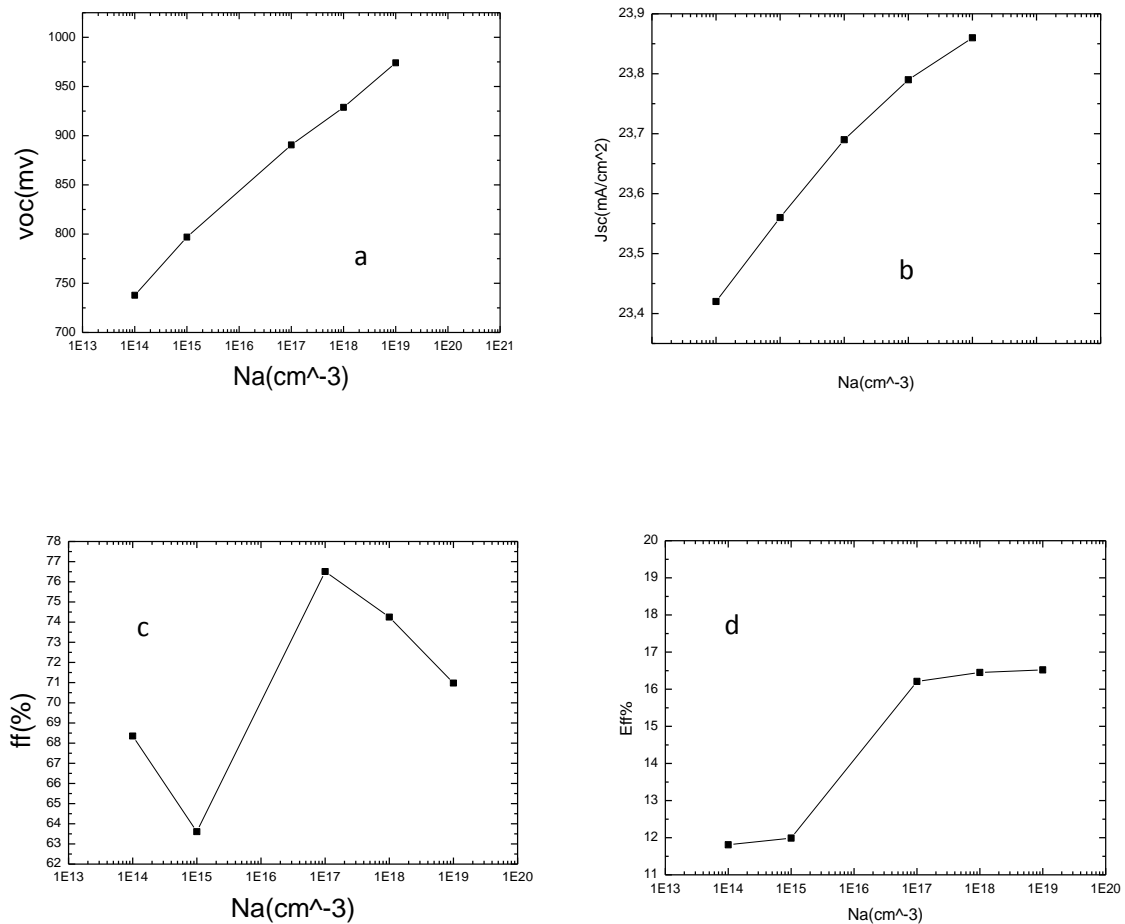


Figure 3.8: the evolution of the open circuit voltage V_{oc} (a), the short circuit current J_{sc} (b), the fill factor FF (c) and the efficiency η (d) as a function of of doping the a-Si:H(p) layer N_a in a tandem solar cell

3.4. Conclusion

In this chapter, we conducted numerical simulations of a-Si:H and a-SiGe:H solar cell and a-Si:H and a-SiGe:H tandem solar cell using the AFORS-Het software, where we focused

Chapter three: results and discussion

on studying the effect of the thickness of the absorber layer and the effect of doping concentration. On the outputs parameters of solar cells, the results showed that the best thickness is 7 μm compared to other thicknesses. The study also showed us that the best value for the efficiency of η in the a-Si:H solar cell is 14.70%, and its value in the a-SiGe:H solar cell is 14.39% and in the tandem solar cell a-Si:H/a-SiGe:H. We reached an efficiency equal to 16.52%. As for the concentration of stimulants, we found For the p type doping, the best conversion efficiency 16.52% for the doping concentration of 10^{19} . For the n type doping, the best conversion efficiency is 25% for the concentration of 10^{20} cm^{-3}



General conclusion

General conclusion

Amorphous semiconductors have garnered significant attention in recent times due to their distinct characteristics and financial benefits, such as their ability to be more affordable than their crystalline counterparts. These materials provide a reasonable alternative in spite of shortcomings including poor mobility, high fault density, and lack of repeatability.

This work focused on the study of hydrogenated amorphous silicon (a-Si:H) solar cells using the AFORS-HET software, which is suitable for this type of cell, to maximize yield by optimizing the cell's characteristic properties. Given that the cell is a multi-layer system, it is necessary to examine each layer and assess the impact of changes in optical and electrical factors on the cell as a whole.

In this work, we simulated a simple n-i-p structure solar cell based on hydrogenated amorphous silicon (a-Si:H) that contains a top layer of a-Si:H n-type, a middle layer of a-Si:H i-type, and a bottom layer of a-Si:H p-type. Then, we studied a solar cell based on amorphous silicon-germanium which contained a top layer of a-SiGe:H n-type, a middle layer of a-SiGe:H i-type, and a bottom layer of a-SiGe:H p-type. Afterwards, we examined a tandem cell consisting of a top layer of a-Si:H n-type, a middle layer of (a-Si:H and a-SiGe:H) i-type, and a bottom layer of a-Si:H p-type. We varied the thickness of the middle intrinsic layer (i) and the doping concentration to observe their effects on the electrical properties. The results showed that the optimal thickness is 7 micrometres compared to other thicknesses. The study also indicated that the optimal efficiency value (η) is 14.70 % for the a-Si:H solar cell, 14.39 % for the a-SiGe:H solar cell, and 16.52 % for the a-Si:H/a-SiGe:H tandem solar cell. Regarding the doping concentration, we discovered that the optimal conversion efficiency for p-type doping is 16.52% at a concentration of 10^{19} cm^{-3} . The optimal conversion efficiency for n-type doping is 25% at a concentration of 10^{20} cm^{-3} .

The results suggest that hydrogenated amorphous silicon and its alloys can form a strong foundation for developing innovative solar cells that meet the increasing demand for clean and renewable energy. Thus, this study provides a comprehensive framework that researchers and engineers can rely on in developing and applying tandem solar cells, contributing to the advancement of solar technology and achieving global environmental goals.



Sources and references

Sources and references

- [1]- كانون خلود, فطيمي عماد, محاكاة خلية شمسية ذات اغشية رقيقة باستعمال برنامج AFORS-HET مذكرة ماستر 2022/2023 , قاصدي مرباح , ورقة
- [2]-https://www.researchgate.net/figure/Direct-diffuse-and-reflected-radiations-of-Solar-irradiation_fig4_362888216
- [3]- https://www.researchgate.net/figure/The-wavelength-range-of-solar-radiation-Elaboration-based-on-4-7-29_fig1_366842064
- [4]- salec selma nasri , Étude et modélisation d'une cellule solaire photovoltaïque à base de silicium , Mémoire de Master 2020/2021 , Université de Ghardaïa
- [5]https://ar.wikipedia.org/wiki/%D8%AE%D9%84%D9%8A%D8%A9_%D8%B4%D9%85%D8%B3%D9%8A%D8%A9
- [6]- <https://www.electronicbub.com/>
- [7]- <https://byjus.com/physics/p-n-junction/>
- [8]- Reciou Meriem , Messahel Halima , Simulation des cellules photovoltaïque pérovskites par le logiciel AFORS-HET, Mémoire de Master 2022/2023, Université de Ghardaïa
- [9]- <https://www.nrel.gov/pv/cell-efficiency.html>.
- [10]-
https://document.environnement.brussels/opac_css/electfile/IF%20ENERGIE%20Mod3%20Fonctionnement%20technologies%20PV%20FR
- [11] - Mr BOUGUENNA Ibrahim Farouk, Modélisation et Optimisation d'une Cellule Solaire Tandem a-Si:H/a-SiGe , Mémoire de magistère, Université des Sciences et de la Technologie d'Oran Mohamed Boudiaf , Oran
- [12]-R. Varache, C. Leendertz, M.E. Gueunier-farret, J. Haschke, D. Muñoz, L. Korte, Investigation of selective junctions using a newly developed tunnel current model for solar cell applications, Solar Energy Materials and Solar Cells, 141 (2015) 14-23.

Sources and references

[13]-kateb,M.N, Etude par simulation numérique d'une cellule solaire en a-Si:H/ μ c-Si:H multijonction ,(2022),doctoral thesis , Mohamed Khider University , Biskra

[14]- S.M. Iftiqar , Junsin Yi ,(2023), Theoretical investigation of silicon thin film solar cell for improving short and long wavelength response, Current Applied Physics volume 50, page 107–116

Sources and references

الجمهورية الجزائرية الديمقراطية الشعبية
République Algérienne Démocratique et Populaire
وزارة التعليم العالي والبحث العلمي
Ministère de l'Enseignement Supérieur Et de La Recherche Scientifique
جامعة غرداية
Faculté des sciences et Technologies
Département d'automatique et
d'électromécanique
كلية العلوم والتكنولوجيا
قسم الآلية والكهروميكانيك
Université de Ghardaïa

غرداية في:

إذن بالطباعة (مذكرة ماستر)

بعد الاطلاع على التصحيحات المطلوبة على محتوى المذكرة المنجزة من طرف الطلبة التالية أسماؤهم:

1. الطالب (ة): شمس الدين الزهر

2. الطالب (ة):

تخصص: ميكانيكا كهربائية و ميكانيكا معدنية

نمنح نحن الأستاذ (ة):

الاسم واللقب	الرتبة - الجامعة الأصلية	الصفة	الامضاء
نعتان بهنا	MAB جامعة غرداية	مصصح (1)	
احمد بن الحاج احمد	MAF جامعة غرداية	مصصح (2)	
دريج العمار صبي	MCA جامعة غرداية	مؤطر	
صالح سراج	MCB جامعة غرداية	رئيس اللجنة	

الإذن بطباعة النسخة النهائية لمذكرة ماستر الموسومة بعنوان

Study and simulation of tandem cell based on hydrogenated amorphous Silicon

إمضاء رئيس القسم

